（表紙）

表　　題　心不全予防におけるβカテニン転写阻害薬の薬効・薬理
(The pharmacotherapeutic effects and molecular mechanism of β-catenin inhibitor for heart failure)

論 文 の 区 分　博士課程

著　　者　　名　ミタターム タナチャイ

担当指導教員氏名　今井　靖　教授

所　　属　自治医科大学大学院医学研究科
専攻　地域医療学系
専攻分野　内分泌代謝疾患・病態解析学
専攻科　臨床薬物治療学

2021年　1月　8日申請 学位論文

Thanachai Methatham

## Contents

Thanachai Methatham

## ACKNOWLEDGEMENTS

I would like to express my deepest gratitude and appreciation to Professor Yasushi Imai for guidance supervision, suggestion, knowledge, and encouragement throughout the study. His expertise in the field of cardiovascular medicine have enlighten and broaden me to obtain the knowledge. I also sincerely thank to Associate Professor Kenichi Aizawa who has been my main mentor throughout my studying period. Without his endless guidance and support, every research of mine would not have been completed. His wisdom, calmness and concentration will be imprinted in my future works.

I am also deeply thankful to Mr. Shota Tomida for their valuable suggestions on the experiments and comments on my manuscript and thesis.

I would like to thank all members of Clinical Pharmacology Laboratory at Jichi Medical University for their help on my experiments. My appreciation also goes to Jichi Medical University for the financial support of Special Student Scholarship and Research Assistance Scholarship, Jichi Medical University. I really appreciate for their management and help from staff of Graduate School of Medicine.

This work has been supported by JMU start-up award from Jichi Medical University. The funder did not play a role in the scheme of study, analyzation, data collection, publication, or manuscript's preparation.

Finally, I am deeply indebted and grateful to my family for their love, understanding, and encouragement throughout my life.

Thanachai Methatham

Thanachai Methatham

## ABSTRACT

Heart failure (HF) is a complex syndrome with enormous socioeconomic burden worldwide and continues to be a main cause of disability, morbidity, and mortality. HF displays the increase in myocyte size and cardiac wall thickness which is found when hypertrophic growth caused by hypertension. ICG001 is a low molecular weight compound that impedes β-catenin-mediated gene transcription. Previously, ICG001 was shown to protect both heart and kidney in cardiorenal syndrome. However, the mechanisms of ICG001 to prevent HF remain unclear. I investigated the preventive roles and mechanisms of ICG001 in transverse aortic constriction (TAC) resulting in cardiac hypertrophy and fibrosis in mice. Four weeks after TAC, the heart weight/body weight (HW/BW) ratio was significantly reduced in mice treated with ICG001. ICG001 attenuated the cardiac hypertrophy in vivo and the extent of fibrosis in the LV wall was decreased. The expression of *Bnp*, *Klf5*, fibronectin, *β-MHC*, and β-catenin was reduced in the TAC mice treated with ICG001, which indicated that ICG001 attenuated cardiac hypertrophy and fibrosis. Moreover, the mRNA expression of multiple inflammatory cytokines secreted by macrophages including *Il4*, *Tgfb1*, and *Ccl2* were significantly decreased in the heart of the ICG001-treated TAC mice. Immunohistochemistry showed decrease in the number of cells expressing a macrophage marker CD68 in the heart of the TAC mice treated with ICG001. Flow cytometry was confirmed the reduction of macrophage accumulation in ICG001-treated TAC mice. In addition, the substrate metabolism provided that ICG001 may mediate the substrates in glycolysis pathway and the distinct alteration of oxidative stress during cardiac hypertrophy and HF. These results illustrate the essential role of ICG001 to prevent HF by attenuating hypertension, cardiac hypertrophy, and cardiac fibrosis as well as macrophage accumulation. Therefore, ICG001

Thanachai Methatham

is a potential drug that can prevent cardiac hypertrophy and fibrosis through reduction of immune activation and alteration of metabolic pathway by inhibition of Wnt/β-catenin signaling.

Thanachai Methatham

**LIST OF FIGURES**

**LIST OF TABLES**

## LIST OF ABBREVIATIONS

| Abbreviation | Definition |
|---|---|
| BCAA | Branched-chain amino acid |
| BNP | Brain natriuretic peptide |
| β-MHC | β-myosin heavy chain |
| BW | Body weight |
| CCL2 | C-C motif chemokine ligand 2 |
| CTGF | Connective tissue growth factor |
| DMSO | Dimethyl sulfoxide |
| EF | Ejection fraction |
| G-1-P | Glucose-1-phosphate |
| G-6-P | Glucose-6-phosphate |
| G-3-P | Glycerol-3-phosphate |
| GSH/GSSG | Reduced and oxidized glutathione |
| HE | Hematoxylin & Eosin |
| HF | Heart failure |
| HR | Heart rate |
| HW | Heart weight |
| IL4 | Interleukin 4 |
| IL10 | Interleukin 10 |
| IVSd | Interventricular septal thickness at end-diastole |
| IVSs | Interventricular septal thickness at end-systole |
| KLF5 | Krüppel-like factor 5 |
| LV | Left ventricular |
| LVESd | Left ventricular end-systolic diameter |
| LVEDd | Left ventricular end-diastolic diameter |
| LVPWd | Left ventricular posterior wall thickness at end-diastole |
| LVPWs | Left ventricular posterior wall thickness at end-systole |
| MT | Masson & Trichrome |
| PPAR- α | Peroxisome proliferator-activated receptor α |
| SDS-PAGE | Sodium dodecyl sulfate polyacrylamide gel electrophoresis |
| TAC | Transverse aortic constriction |
| TGF-β | Transforming growth factor beta |
| TNF-α | Tumor necrosis factor alpha |
| T-PER | Tissue Protein Extraction Reagent |
| WT | Wild type |

Thanachai Methatham

# CHAPTER I

## INTRODUCTION

Heart failure (HF), is a significant health problem that continues to have high mortality. The disability caused by HF presents a substantial burden in society and affects the healthcare system[1]. Hypertension, myocardial infarction (MI), ischemia, and vascular disease cause an increase in myocyte size and cardiac wall thickness, indicating hypertrophy[2]. The heart compensates by increasing its size, but when cardiac hypertrophy exists, it sometimes leads to maladaptation.

Transverse aortic constriction (TAC) is frequently performed to be the most common surgical operation's models to study the adverse cardiac remodeling upon pressure overload[3]. TAC causes left-sided HF because of pressure overload and results in partial occlusion creating stenosis in the aortic arch. A permanent constriction placing around the transverse aorta limited the outflow and created pressure overload in left ventricle (LV). The constriction is created by tying knots over a blunt needle of commonly reported needle diameter, 27 gauge, alongside the aorta[4,5,6]. TAC is a very useful tool to study mechanisms of cardiac hypertrophy and development of HF. It can be used to be the disease progression's model and to study the efficacy of heart treatments (Figure A1).

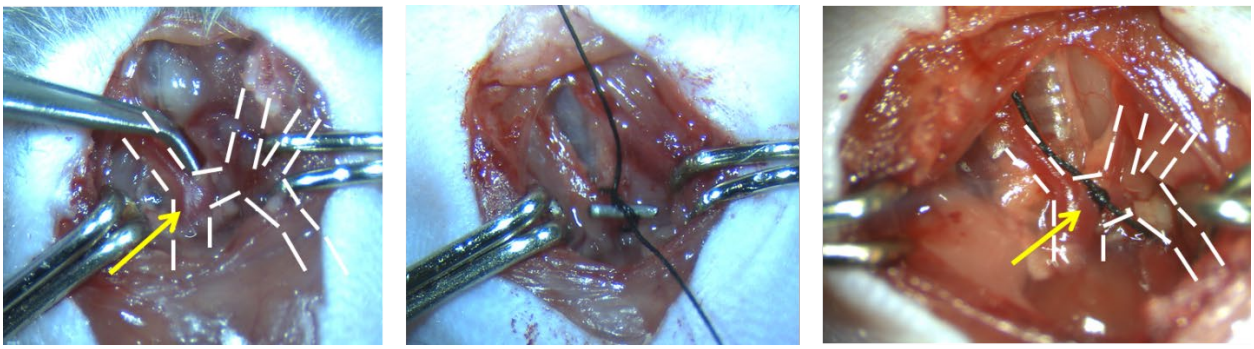

**Figure A1:** Transverse aortic constriction (TAC) by using needle 27 gauge alongside the aorta

Cardiac fibroblasts, critical regulators of the basal structure of the heart, were the predominant cell type which produced the collagen in pathologic cardiac fibrosis. Cardiac fibrosis caused by cardiac injury could disrupt the cardiac conduction, reduced the cardiac output and also increased fibrillar collagen which resulting in HF[7,8,9]. Cardiac fibroblasts play a crucial role by producing proteins to prevent the damage of heart after heart injury. The accumulation of extracellular matrix (ECM) producing by cardiac fibroblasts was an influential modulator of the growth and cell function in heart, but the fibrosis caused by the immoderate production and accumulation of ECM proteins in the cardiac muscle which formed a network of protein around cells results in stiffening in the cardiac tissue and decreased cardiac function which making adverse effects on cardiac structure and function[10,11,12]. Cardiac fibroblasts were the core of proteins that cause cardiac fibrosis[12]. Cardiac fibrosis was occurred after heart injury or inflammation[11]. Krüppel-like factor 5 (KLF5) is one of the Krüppel-like transcription factor which plays an important role to modulate the phenotype of myofibroblasts and smooth muscle cells[13]. KLF5, known as a zinc finger-containing transcription factor, was informed to be crucial in the progress and preservation of the lung, aorta, and heart system[14]. It was reported that the cardiac hypertrophy and fibrosis in the Ang II model were reduced in heterozygous knockout of KLF5[15]. While it was found that KLF5 activated insulin-like growth factor 1 (IGF-1), the mediator in the crosstalk between cardiac fibroblasts and cardiomyocytes, secreted from cardiac fibroblasts. TAC induced the upregulation of KLF5 expression and KLF5 controlled cardiac fibroblasts which played an important role in the myocardial adaptive response to pressure overload[16,17]. *Klf5* haploinsufficiency suppressed cardiac fibrosis and hypertrophy after pressure overload, whereas the alteration of hypertrophic responses was not found in cardiomyocyte-specific Klf5 deletion[16].

On the other hand, cardiac hypertrophy and fibrosis were reduced in cardiac fibroblast-specific Klf5 deletion, indicating that cardiac fibroblasts are required for cardiomyocyte hypertrophy and KLF5 in fibroblasts is important for the response to pressure overload[16]. Furthermore, KLF5 controls the phenotype and function of macrophages. *Klf5* haploinsufficiency showed the decrease of M1 macrophage accumulation in response to unilateral ureteral obstruction[18]. KLF5 controls macrophage polarity in chronic inflammatory diseases[17].

The activation and deposition of macrophages in the heart were shown to be the development of an innate immune response[19]. The study of heart disease showed the activation of the response of inflammatory cytokine resulting in deleterious effect's continuation of the heart by leading to progression of LV dysfunction and HF[20]. Inflammatory genes and cell infiltration were found in the heart of the TAC mice[21,22]. Releasing proinflammatory cytokines and growth factors by macrophages played an important role in LV inflammation and remodeling. The chronic systemic inflammation causing by obesity and hypertension implicated the excess macrophage activation and M1 polarization which release proinflammatory cytokines resulting in impair cardiac function[23]. Proinflammatory circulating monocytes and cytokines are increased in patients with hypertension and continue to rise during symptomatic HF. The expansion of cardiac macrophage is a feature of the transition to HF. The myocardial monocyte infiltration and macrophage accumulation did not occur until HF symptoms have developed in patients with hypertension and in hypertensive mouse models[23]. Macrophages and T-cells were accumulated and increased in the heart after TAC within days to weeks of TAC related to the fibrosis and adverse ventricular remodeling[24,25,26,27,28]. Clearly, mice after TAC will be found the accumulation of macrophages and T-cells and also be found the fibrosis in response to pressure overload. Previous studies suggested that there were several mechanisms which illustrate the induction of

cytokines and subsequent infiltration of protein-inflammatory macrophages in pressure-overloaded myocardium[29].

Previous works showed that KLF5 promoted the cardiac hypertrophy, controlled macrophage and also regulated the expression of peroxisome proliferator-activated receptor α (PPAR-α)[30,31]. The function of PPAR-α has recently been studied in relation to cardiac inflammation and hypertrophy[32]. PPAR-α null mice exhibited cardiac fibrosis in an age-dependent manner and showed the disability to compensate the cardiac functions[33,34]. Inactivation of PPAR-α in animal studies may conduce to change the phenotype and response to pressure overload by cardiac growth indicating that compromise of PPAR-α activity may be the factor related to the change from compensated LV hypertrophy to HF in hypertensive heart disease[35,36]. The administration of PPAR-α activators to aged mice elicited a number of biologic changes including inflammation, glucose homeostasis, and cell differentiation[37]. PPAR-α belongs to the nuclear receptor superfamily and is the ligand of dependent transcription factors which is the key transcriptional regulators controlling the competency of myocardial mitochondrial fatty acid oxidation (FAO)[38,39]. In the regulation of FAO, a main source of ATP in high energy-consuming organs and tissues, PPAR-α was an important factor relating with the energetics[40]. PPAR-α played a critical role in metabolic regulatory processes, particularly in heart muscle[41]. Activating PPAR-α transcription improved the function and energetics of the heart[39].

The multiple energy substrates that provides high energy to the heart are derived from fatty acids, glucose, ketones and amino acids[42,43]. Fatty acid oxidation and glucose metabolism are the main metabolic pathways in the normal heart[44]. Fatty acid oxidation produces the highest energy (40 to 60% of the energy produced in the heart) while carbohydrates metabolism provides only 20 to 40%[43]. Heart failure is accompanied by impaired metabolic flexibility and disturbance of energy

metabolism[43]. In the heart failure, the heart switches from fatty acid oxidation to glucose metabolism to produce energy[43,45]. The switch to glucose metabolism is associated with impaired metabolic flexibility which characterizes the failing heart[46].

Wnt/β-catenin pathway has been focused as one of the key mechanisms in the pathogenesis of HF and it involved in development of organ, tissue remodeling, repair of injury, and inflammation[47,48,49]. The Wnt/β-catenin signaling system played a greatly essential role for development of heart and also was acknowledged to play a critical role in exhibition of cardiac injury response[50]. An evolutionarily conserved signaling pathway of Wnt/β-catenin was involved in injury repair, inflammation and tissue remodeling[47,48,51]. ICG001 was known as a small molecule inhibitor that principally impedes β-catenin-mediated gene transcription. Administration of ICG001, inhibition of the β-catenin, improved the ejection fraction of rats at 10 days post–myocardial infarction[52]. Recently, the role of ICG001 to mediate the injury of heart and kidney implied that the effect of ICG001 to inhibit β-catenin could be a new procedure to protect both heart and kidney in the remedy of cardiorenal syndrome's patients[53]. However, the question of how ICG001 prevent the transition from hypertrophy to HF and the mechanisms of ICG001 by which the heart adapts to prevent HF are still not well defined.

In this study, I investigated the cardiac function, cardiac markers and fibrosis expression, T cell and macrophage accumulations, and the substrate metabolism in mouse model of pressure overload inducing cardiac hypertrophy and fibrosis. I displayed that ICG001 can prevent HF from cardiac hypertrophy and fibrosis due to pressure overload by inhibition of Wnt/β-catenin signaling involved in reduction of KLF5 expression and macrophage recruitment. In addition, this study reveals the novel mechanism associated with reduction of oxidative stress via metabolic alteration.

# CHAPTER II

## OBJECTIVES

Previously, ICG001 was shown to protect both heart and kidney in cardiorenal syndrome. However, the mechanisms of ICG001 to prevent HF remain unclear. Here, I investigate the beneficial roles and precise mechanisms of ICG001 to prevent HF in mice induced by transverse aortic constriction.

# CHAPTER III

# MATERIALS AND METHODS

## 4.1 Materials

### 4.1.1) Antibodies

Anti-CD68 antibody (Abcam, Cat. Ab125212)

Anti-CD3 antibody (SP7) (Abcam, Cat. Ab16669)

Anti-GAPDH (Thermo Scientific, Cat. AM4300)

CD16/32 antibody (BioLegend, TrueStain FcX™)

Anti-mouse CD45 antibody (BioLegend, Alexa Fluor® 700)

Rat IgG2b, κ Isotype Ctrl antibody (BioLegend, Alexa Fluor® 700)

Anti-mouse CD3ε (BioLegend, FITC)

Armenian Hamster IgG Isotype Ctrl Antibody (BioLegend, FITC)

Anti-mouse Ly-6C antibody (BioLegend, FITC)

Rat IgG2c, κ Isotype Ctrl Antibody (BioLegend, FITC)

Anti-mouse/human CD11b antibody (BioLegend, Pacific Blue™)

Rat IgG2b, κ Isotype Ctrl Antibody (BioLegend, Pacific Blue™)

Anti-mouse F4/80 antibody (BioLegend, PE/Cyanine7)

Rat IgG2a, κ Isotype Ctrl Antibody (BioLegend, PE/Cyanine7)

Anti-mouse CCR2 APC-conjugate antibody (R&D systems)

Rat $IgG_{2B}$ Isotype Control (R&D systems)

Anti-PPAR alpha antibody (Abcam, Cat. Ab215270)

Anti-β-catenin (BD bioscience Cat. 610154)

#### 4.1.2) Chemicals and reagents

Anti-mouse Ig, κ/Negative control compensation particle set (BD bioscience)

Anti-Rat and Anti-Hamster Ig κ /Negative Control Compensation Particles Set (BD bioscience)

Dimethyl sulfoxide (DMSO) (Sigma Aldrich)

ICG001 (β-Catenin/Tcf Inhibitor V) (Merck)

Fixative solution (Sakura Finetek Japan Co., Ltd)

Phosphate buffered saline (PBS) (Takara)

Clarity Western ECL substrate (Bio rad)

Carrazi's hematoxylin solution (Muto Pure Chemicals, Ltd., Tokyo, Japan)

Eosin solution (Wako Pure Chemical Industries, Ltd)

Ethanol (Kanto Chemical Co. Inc., Japan)

Xylene (Wako)

VectaMount™ permanent mounting medium (Vector laboratories)

BLOXALL® endogenous blocking solution (Vector laboratories)

Vectastain® Elite ABC-HRP Kit Peroxidase (Rabbit IgG) (Vector laboratories)

ImmPACT™ DAB peroxidase substrate (Vector laboratories)

RNeasy mini kit (QIAGEN)

RNase-Free DNase digestion (QIAGEN)

ReverTra Ace® *reverse transcriptase* (Toyobo)

SYBR Premix Ex Taq II Kit (RR820A; Takara Biotechnology)

T-PER® tissue protein extraction reagent (Thermo Scientific)

Protease inhibitors (Thermo Scientific Halt Protease Inhibitor Cocktail and EDTA-Free)

Pierce™ BCA protein assay kit (Thermo Scientific)

Precision Plus Protein™ Dual color Standards marker (Bio-Rad Laboratories)

Collagenase type IV (Wothington Biochemical Corporation)

Dispase II (Sigma-Aldrich)

Dulbecco's phosphate buffered saline no calcium, no magnesium (DPBS) (Thermo Scientific)

Hanks' Balanced Salt Solution no calcium, no magnesium (HBSS) (Thermo Scientific)

Tris buffered saline with tween (Cell signaling)

iBlot 2 PVDF mini stacks (Invitrogen)

NuPAGE SDS Running buffer (Invitrogen)

NuPAGE 10% Bis-Tris Gel 1.5 mm x 15 wells (Invitrogen)

Phos stop™ pkg of 20 tablets (Sigma Aldrich)

Complete ™ Mini, EDTA-free Protease inhibitor cocktail 25 tablets (Sigma Aldrich)

Isoflurane (Pfizer)

Signagel, electrode gel (Parker Laboratories)

Isoflow sheath fluid (Beckman coulter)

Medetomidine (ZENOAQ)

Midazolam (SANDOZ)

Butanol tartrate (Meiji Seica)

#### 4.1.3) Equipments

Amicon® Ultra Centrifugal filters 3K (Merck)

Echocardiography Vevo® 2100 Imaging System (FUJIFILM VisualSonics, Canada)

Keyence BZ-9000 microscope

Nanodrop1000 (Thermo Fisher Scientific)

Stratagene Mx3005P QPCR System (Agilent Technologies, Santa Clara, California, USA)

Thanachai Methatham

Thermo Alumi Bath (Iwaki, ABL-121)

Sony SH800 flow cytometer

FlowJo (FlowJo, LLC)

40 μm cell strainer (Falcon)

TAITEC Ve-125 Centrifugal Concentrator

Liquid Chromatography Mass Spectrometry 8030 and 8050 (LCMS8030 and 8050) (Shimadzu)

0.2 ml, 96-well PCR plate Non-skirt, clear (WATSON)

iBlot™ 2 Gel Transfer Device (Thermo Scientific)

Fujifilm LAS-3000 Imager (Fuji)

ChemDoc Touch (BioRad)

## 4.2 Methods

### 4.2.1) Animals and pressure overload model

This study utilized 8-week-old male mice (C57BL/6 commercially purchased from Takasugi Experimental Animal Supply Co., Ltd., Japan). The Institutional Animal Care and Concern Committee at Jichi Medical University approved the experiments of mice and all selected mice were used according to the committee's guidelines. These mice were allowed to consume food and water under a 12 h light and dark cycle in a room with controlled temperature and humidity conditions. We used TAC model to induce pressure overload in mice. Furthermore, they were randomly assigned to either TAC group or sham surgery group. Briefly, they were anesthetized with medetomidine (1 mg/ml), midazolam (5 mg/ml), and butanol tartrate (5 mg/ml) and underwent a longitudinal incision along the proximal portion of the sternum. We placed a 27-gauge needle on the aorta and ligated over the needle using 6-0 silk suture to yield a narrow

diameter at the aortic arch. After the ligation, we removed the needle from the ligation area. The sham group also underwent a similar procedure but without ligation.

#### 4.2.2) Echocardiography

Echocardiography was performed before and at 4 weeks after TAC or sham surgery. Briefly, all mice were placed on the heating plate in a supine position, with the extremities tied to the plate by four electrocardiography leads. The fur on the chest was removed using a hair remover cream, and the visibility of the cardiac chambers was improved by applying an ultrasound gel on the thorax area. After the mice were anesthetized with 5% of induction phase and 1.5% of maintenance phase of isoflurane, echocardiography was performed using Vevo2100 equipped with a 30 MHz linear transducer. For data collection, we measured the following factors: interventricular septal thickness at end-diastole (IVSd), interventricular septal thickness at end-systole (IVSs), LV posterior wall thickness at end-diastole (LVPWd), LV posterior wall thickness at end-systole (LVPWs), LV end-systolic diameter (LVESd), LV end-diastolic diameter (LVEDd), and heart rate (HR). We calculated the EF and captured its images to measure wall thickness. The formula to calculate the EF was 100 * ((LV Vol;d – LV Vol;s)/LV Vol;d). Measurements and analyses were conducted by two individuals who were blinded to the experimental groups of mice. Then, the mice were sacrificed to collect their blood and heart tissue samples.

#### 4.2.3) Treatments

After TAC surgery, the mice were randomly separated into two groups, namely, vehicle group (negative control) and ICG001-treated TAC group. ICG001 (50 mg/kg/day) was intraperitoneally administered for 10 days (twice per day) to evaluate its effect on cardiac function. For the vehicle

group, vehicle (DMSO) was intraperitoneally administered into the following subgroups: sham and wild-type groups. EF was measured again at 4 weeks after the completion of administration. Then, we collected the heart and blood samples and measured the body weight to compare the HW/BW ratio (mg/g). Thereafter, the LV tissues were collected for further experiments.

#### 4.2.4) Histology

Heart samples were collected at indicated time points after TAC surgery. After phosphate-buffered solution (PBS) perfusion through the LV, the hearts were washed by cold PBS and fixed for 24 h in a rapid fixative solution (Sakura Finetek Japan Co., Ltd.). Tissues were embedded in paraffin and sliced into sections (5 μm). The sections were transferred onto microscope slides and stained with Hematoxylin and eosin (HE) stain to evaluate the cardiomyocyte cross-sectional area and Masson's trichrome (MT) stain to assess the extent of fibrosis. Briefly, 5 μm-thick sections were deparaffinized and rehydrated. We used the standard method for HE staining. The sections were incubated in Carrazi's hematoxylin solution (Muto Pure Chemicals, Ltd., Tokyo, Japan) for 5 min and washed in tap water. Then, they were differentiated in 1% acid alcohol and dehydrated in 95% ethanol, followed by incubation in eosin solution (Wako Pure Chemical Industries, Ltd) for 3 min and dehydration in a series of ethanol (80%, 95%, and 100%). For MT stain, after deparaffinization and rehydration, the sections were incubated in 10% trichloroacetic acid solution mixed with potassium dichromate (ratio 1:1) for 15 min and washed in tap water for 3 min. Then, they were incubated in Weigert's hematoxylin for 5 min and washed in running tap water and rinsed with distilled water. After that, they were placed in Biebrich scarlet for 5 min and washed for 5 sec. Then, they were incubated in solution II (phosphomolybdic acid hydrate mixed with tungsto (VI) phosphoric acid n-hydrate (1:1)) for 30 min and washed in tap water for 5 sec.

Next, they were placed in aniline blue for 5 min and washed in tap water for 5 sec. Then, they were placed in 1% acetic acid and washed in tap water for 5 sec. After that, they were dehydrated in a series of ethanol (80%, 95%, and 100%). Finally, they were cleared in xylene for 10 min and mounted with VectaMount™ (Vector). Histopathological features of each section were examined under the Keyence BZ-9000 microscope to show the pathological change of heart size and fibrosis. The area of fibrosis was analyzed by ImageJ.

#### 4.2.5) Immunohistochemistry

We sliced 5 μm-thick sections of paraffin-embedded hearts and transferred them onto microscope slides. These sections were deparaffinized and rehydrated using xylene and graded alcohol series and then washed for 5 min in tap water. Next, they were heated in citric acid in a microwave for 8 min. The tissues were subsequently quenched with BLOXALL® blocking solution for 10 min and washed in PBS buffer for 5 min. The sections were processed using the Vectastain® Elite ABC-HRP Kit Peroxidase (Rabbit IgG) (Vector Labs, Cat. PK-6101) and ImmPACT™ DAB peroxidase substrate (Vector) following the manufacturer's protocol. Briefly, these sections were blocked with diluted normal goat serum for 20 min to block nonspecific binding. Next, some sections were incubated overnight with anti-CD68 antibody (Abcam, Cat. Ab125212) at 1:1,000 dilution to detect macrophage accumulation, while the others were incubated overnight with anti-CD3 antibody (SP7) (Abcam, Cat. Ab16669) at 1:500 dilution to detect T cell accumulation. Furthermore, the sections were washed with PBS buffer for 5 min and incubated with diluted biotinylated secondary goat anti-rabbit IgG for 30 min. Next, they were washed again with PBS buffer for 5 min and then incubated with Vectastain Elite ABC reagent for 30 min, followed by another 5 min wash with PBS buffer. These sections were applied with ImmPACT™ DAB

peroxidase substrate (Vector) for 2 min and then rinsed with distilled water. Afterward, they were counterstained with hematoxylin for 4 min, washed with distilled water, dehydrated with 70%, 80%, 90%, and 100% ethanol, cleared in xylene, and mounted in VectaMount™ (Vector). Images were captured using BZ-9000 (KEYENCE). The intensity of macrophage and T cell was analyzed by ImageJ.

#### 4.2.6) RNA extraction and real-time PCR

After PBS perfusion through the LV, heart tissues were collected and washed in cold PBS following TAC. We extracted RNA from the LV tissues of mice by using RNeasy mini kit (QIAGEN, Cat. 74106) and removed DNA contamination by RNase-Free DNase digestion (QIAGEN, Cat. 79254) in accordance with the manufacturer's protocol. The RNA was washed and eluted, and RNA concentration and purification were assessed with Nanodrop1000 (Thermo Fisher Scientific). According to the manufacturer's protocol, cDNA was synthesized by ReverTra Ace® reverse transcriptase (Toyobo). Real-time PCR was conducted using the SYBR Premix Ex Taq II Kit (RR820A; Takara Biotechnology) and the Stratagene Mx3005P QPCR System (Agilent Technologies, Santa Clara, California, USA). First, in the total reaction system, 25 μl was added to 2 SYBR Premix Ex Taq II (12.5 μl), cDNA (2 μl), 10 μmol/L concentration of forward primer (1 μl), 10 mmol/L concentration of reverse primer (1 μl), and RNase-free water (8.5 μl). Moreover, after the initial denaturation at 95 °C for 30 sec, the mixtures were denatured at 95 °C for 5 sec, and annealed and extended at 60°C for 30 sec according to the manufacturer's protocol. The cycle of denaturation, anneal and extension was repeated for 40 times. Following the real time PCR, a melting curve was created by gradually increasing the temperature to 95 °C to test the homogeneity of PCR product. This experiment used the comparative cycle threshold (CT) method which is a

form of relative quantitation, comparing the levels of a target gene in test samples or unknown samples relative to a sample of reference or calibrator. Real-time PCR was run in 96-well plates, and the relative expression levels of the target genes were evaluated after normalizing against the GAPDH gene and quantified using the comparative CT method. The comparative quantitation module in MxPro™ Software was used to calculate relative quantity for gene expression experiments. Table 1 lists the specific gene primer sequences.

**Table 1:** Primers for real time polymerase chain reaction

| Gene | Forward primer (5'-3') | Reverse primer (5'-3') | Ref |
|---|---|---|---|
| BNP | ATGGATCTCCTGAAGGTGCTG | GTGCTGCCTTGAGACCGAA | [54] |
| β-MHC | CCGAGTCCCAGGTCAACAA | CTTCACGGGCACCCTTGGA | [55] |
| β-catenin | TCAAGAGAGCAAGCTCATCATTCT | CACTTTCAGCACTCTGCTTGTG | [53] |
| CTGF | TGTGTGATGAGCCCAAGGAC | AGTTGGCTCGCATCATAGTTG | [55] |
| Collagen I | TGGCCTTGGAGGAAACTTTG | CTTGGAAACCTTGTGGACCAG | [55] |
| Fibronectin | CGAGGTGACAGAGACCACAA | CTGGAGTCAAGCCAGACACA | [53] |
| GAPDH | GGTGCTGAGTATGTCGTGGA | ACAGTCTTCTGGGTGGCAGT | [53] |
| IL-4 | GGTCTCAACCCCCAGCTAGT | CCGATGATCTCTCTCAAGTGAT | [56] |
| IL-10 | GATGCCCCAGGCAGAGAA | CACCCAGGGAATTCAAATGC | [56] |
| KLF5 | TGGTTGCACAAAAGTTTATAC | GGCTTGGCGCCCGTGTGCTTCC | [16] |
| PPAR-α | TGCAAACTTGGACTTGAACG | GATCAGCATCCCGTCTTTGT | [57] |
| TGF-β | CTCCCGTGGCTTCTAGTGC | GCCTTAGTTTGGACAGGATCTG | [56] |
| TNF-α | CAGCCGATGGGTTGTACCTT | GGCAGCCTTGTCCCTTGA | [56] |
| Ccl2 | GTCTGTGCTGACCCCAAGAAG | TGGTTCCGATCCAGGTTTTTA | [56] |

| | | | |
|---|---|---|---|
| Wnt1 | GCCCTAGCTGCCAACAGTAGT | GAAGATGAACGCTGTTTCTCG | [58] |
| Wnt3a | TTCTTACTTGAGGGCGGAGA | CTGTCGGGTCAAGAGAGGAG | [58] |

#### 4.2.7) Western blotting

Using T-PER® tissue protein extraction reagent (Thermo Scientific, Cat. 78510), we extracted proteins from the cardiac tissues. Briefly, the protease inhibitors (Thermo Scientific Halt Protease Inhibitor Cocktail and EDTA-Free) were added to the T-PER reagent before use. The appropriate amount of T-PER reagent was added to the tissue sample and then homogenized. Thereafter, the sample was centrifuged at 10,000 × g for 5 min to cell pellets. Next, we collected the supernatant and quantified the protein concentration by using Pierce™ BCA Protein Assay Kit (Thermo Scientific, Cat. 23225) according to the manufacturer's protocol. Protein samples were mixed with 5X loading buffer and denatured in Thermo Alumi Bath (Iwaki, ABL-121) for 10 min. Then, they were cooled and stored at −80°C for further study. Equal amounts of protein from each sample and Precision Plus Protein™ Dual color Standards marker (Bio-Rad Laboratories, Cat. 1610374) were fractionated by sodium dodecyl sulfate polyacrylamide gel electrophoresis (SDS-PAGE). The proteins were transferred from SDS-PAGE to the membrane by a gel-transfer device (iBlot™ 2 Gel Transfer Device). Afterward, the membrane was incubated with different primary antibodies for 1 h and then with secondary antibodies for another 1 h, at room temperature. The blots were scanned with an infrared imaging system (Fujifilm LAS-3000 Imager and ChemDoc Touch) to quantify the expression of protein. The protein expression levels were normalized to the corresponding GAPDH (Thermo Scientific, Cat. AM4300) levels. The expression level of each target protein was calculated by dividing the difference of intensity of the target protein and the intensity of background by the difference of the intensity of GAPDH and the intensity of

background.

#### 4.2.8) Flow cytometry

Heart tissues were minced into small pieces and digested with collagenase type IV (2 mg/ml) (Wothington Biochemical Corporation) and dispase II (1.2 U/ml) (Sigma-Aldrich) in the Dulbecco's phosphate buffered saline supplemented with 0.9 mmol/L $CaCl_2$. Then, heart tissues were incubated at 37 ºC for 15 min with gentle rocking. Next, heart tissues in digestion buffer were triturated by 10 ml serological pipette for 10 times after incubation. Suspension of heart tissues were incubated at 37 ºC for 15 min again and then triturated twice again. After that, they were placed on ice. The cell suspensions were then filtered by 40 μm cell strainner. Filtered suspensions were placed with 30 ml of Dulbecco's phosphate buffered saline in 50 ml tubes and centrifuged to collect the cell at 2,500 rpm for 20 min. Then, 250 ml 2% FCS/HBSS solution were added to resuspend cell pellets and blocked with the CD16/32 antibody (BioLegend, TrueStain FcX™) at 4 ºC for 1 h. After that, cells were stained with primary antibodies in FACS buffer: anti-mouse CD45 antibody (BioLegend, Alexa Fluor® 700), anti-mouse CD3ε (BioLegend, FITC), anti-mouse Ly-6C antibody (BioLegend, FITC), anti-mouse/human CD11b antibody (BioLegend, Pacific Blue™), anti-mouse F4/80 antibody (BioLegend, PE/Cyanine7), anti-mouse CCR2 APC-conjugate antibody (R&D systems) and incubated at 4 ºC for 30 min in the dark. Next, the analysis of flow cytometry was performed by Sony SH800 flow cytometer and analysed with FlowJo program (FlowJo, LLC).

#### 4.2.9) Mass spectrometry

Heart samples from each group were randomly selected for metabolomics analysis. The heart

sample were removed from the mice and were put in liquid nitrogen instantly for freezing and were kept at −80 °C until use. Each heart sample (30-50 mg) was homogenized in 500 µl of inner standard for Liquid Chromatography Mass Spectrometry (LCMS) and added the ultrapure water 250 µl after homogenization. Then, the homogenized samples were collected and added 400 µl of chloroform and the mixture was mixed thoroughly. The homogenization was centrifuged at 15,000 *rpm* for 15 min at 4°C. Next, the supernatant was collected and filtered by 0.5 ml Amicon® Ultra Centrifugal filters 3K. Then, the filtrate was centrifuged at 15,000 *rpm* for 90 min at 4°C. After that, the filtrate was lyophilized by TAITEC Ve-125 Centrifugal Concentrator for overnight. Then, all samples were added 100 µl of ultrapure water and processed to LCMS. LCMS was conducted using a Liquid Chromatography Mass Spectrometry 8030 and 8050 (LCMS8030 and 8050) (Shimadzu).

#### 4.2.10) Statistical analysis

Statistical significance of distributed data was analyzed by Log-rank (Mantel-Cox) and by one-way or two-way ANOVA followed by Tukey's test for multiple comparisons. The statistical test used in each experiment is indicated in the figure legends. All analyses were computed using the GraphPad Prism 6 software. P values less than 0.05 were considered significant.

# CHAPTER IV

# RESULTS

## 1. ICG001 increases survival of mice with HF and maintains cardiac function after TAC

I used the TAC mouse model to induce LV pressure overload causing the cardiac hypertrophy and HF. From ten days after TAC to one month, TAC mice seldom died. After TAC, the ICG001 (50mg/kg/day) was intraperitoneally administered for 10 days (twice per day) in ICG001-treated TAC mice group (Fig. 1A). Up to four weeks after TAC operation, mice started to die because of acute HF due to pressure overload and all of mice died within 7 weeks after TAC, whereas ICG001 treatment after TAC increased survival to 12 weeks (Fig. 1C). It showed that ICG001 treatment significantly improved the survival rate in mice with establishing the LV pressure overload-induced HF. Survival curve analysis showed all TAC mice with 27 gauge died within 7 weeks after TAC operation suggesting that all of mice subjected to TAC with 27 gauge suffered from HF. To investigate the prevention against TAC-induced cardiac hypertrophy by protective effect of ICG001, the echocardiography was checked to determine the function of heart (Fig. 1B). To elucidate whether ICG001 may protect the function of pressure-overloaded heart, ICG001 and DMSO (negative control) were intraperitoneally administered and EF was measured again after completion of administration. Four weeks after TAC, the mice showed significantly decreased EF in vehicle group compared with ICG001-treated TAC mice group (Fig. 1D). The EF in mice treated with ICG001 was higher than vehicle group after TAC. It means that ICG001 improved the value of EF in ICG001-treated TAC mice. Moreover, the echocardiography demonstrated the significant increase of left ventricular internal dimension at end-systole (LVIDs), left ventricular internal dimension at end-diastole (LVIDd), and left ventricular mass corrected (LV mass corrected) in

TAC mice compared with ICG001-treated TAC mice group (Fig. 1E-G, Table 2). To investigate the activation of Wnt/β-catenin signaling under pressure overload induced cardiac lesions, I examined the gene expression of Wnt ligands including Wnt1 and Wnt3a in heart of TAC mice. Four weeks after TAC, both of genes notable increase in TAC mice (Fig. 1J-K). This finding was confirmed that Wnt/β-catenin was activated in mice subjected to TAC. As shown in Fig. 1H-I, real-time reverse transcriptase-polymerase chain reaction (qRT-PCR) showed the levels of markers of HF including brain natriuretic peptide (*Bnp*) and β-myosin heavy chain (*β-MHC*) were also significant reduced in TAC mice treated with ICG001 compared with TAC mice. These data indicate that the cardiac function was maintained after TAC and treated with ICG001.

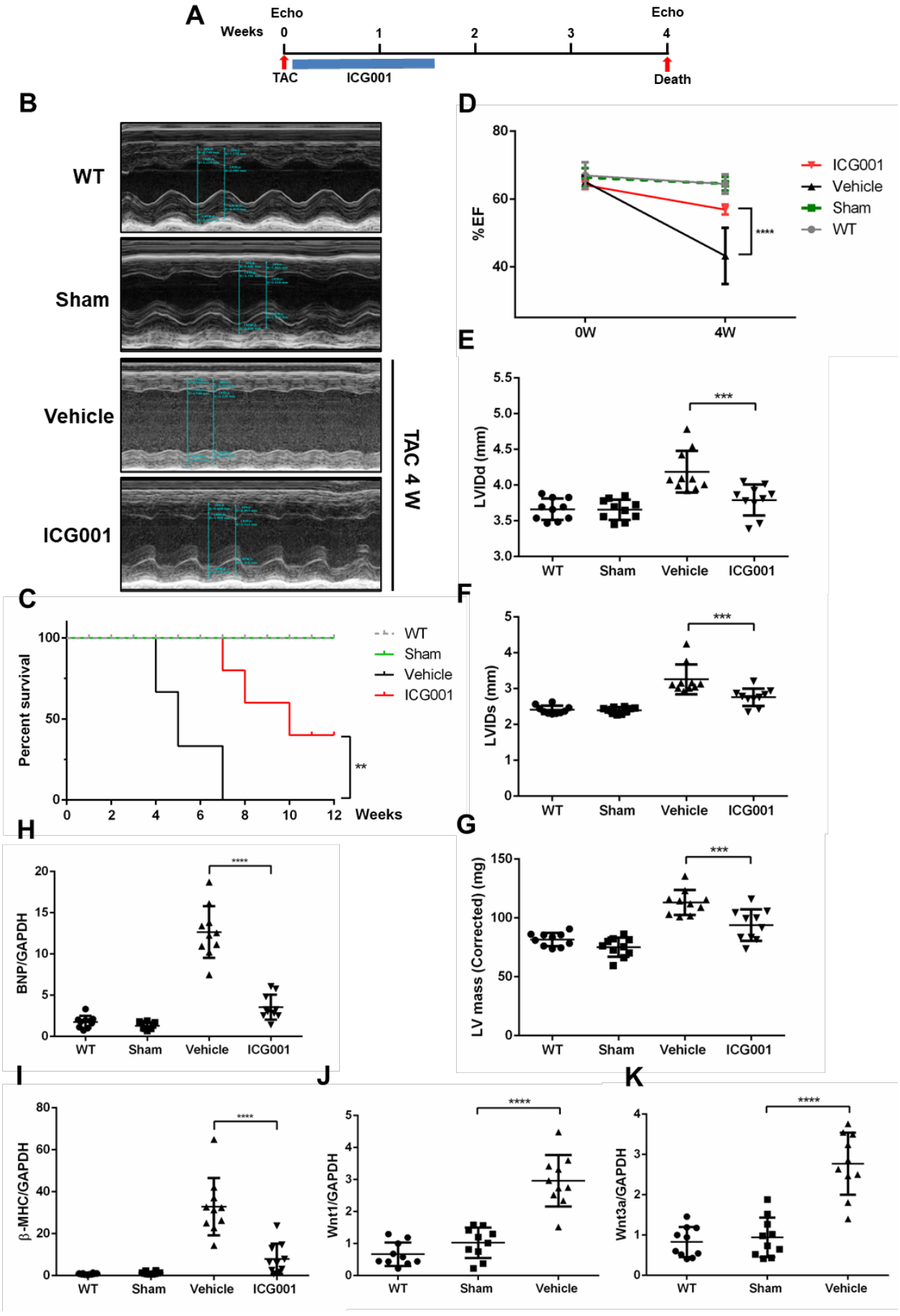
A
Echo
Weeks 0 1 2 3 4
Echo
TAC
ICG001
Death
B
WT
Sham
Vehicle
ICG001
TAC 4 W
D
%EF
80
60
40
0W
4W
****
ICG001
Vehicle
Sham
WT
E
LVIDd (mm)
5.5
5.0
4.5
4.0
3.5
3.0
***
WT
Sham
Vehicle
ICG001
C
Percent survival
100
50
0
0 2 4 6 8 10 12 Weeks
**
WT
Sham
Vehicle
ICG001
F
LVIDs (mm)
5
4
3
2
1
0
***
WT
Sham
Vehicle
ICG001
H
BNP/GAPDH
20
15
10
5
0
****
WT
Sham
Vehicle
ICG001
G
LV mass (Corrected) (mg)
150
100
50
0
***
WT
Sham
Vehicle
ICG001
I
β-MHC/GAPDH
80
60
40
20
0
****
WT
Sham
Vehicle
ICG001
J
Wnt1/GAPDH
5
4
3
2
1
0
****
WT
Sham
Vehicle
K
Wnt3a/GAPDH
4
3
2
1
0
****
WT
Sham
Vehicle

**Figure 1:** ICG001 increases survival of mice with HF and maintains cardiac function after TAC. (A) Experimental design. (B) Example of M-Mode echocardiography of left ventricle at 4 weeks after TAC. (C) Survival curves showed that mortality rate was significantly ameliorated in ICG001 treated TAC mice compared with TAC mice (n=10 in each group). (D) Left ventricular ejection fraction (LVEF), (E) left ventricular internal dimension at end-diastole (LVIDd), (F) left ventricular internal dimension at end-systole (LVIDs), and (G) left ventricular mass corrected (LV mass corrected) after TAC 4 weeks showed systolic dysfunction and ICG001 maintains cardiac function after TAC. (H-I) real time polymerase chain reaction of brain natriuretic peptide (*BNP*) and β-myosin heavy chain (*β-MHC*) was induced after TAC and ICG001 reduced their expression after TAC. (J-K) real time polymerase chain reaction showed the Wnt genes, Wnt1 and Wnt3a, was induced in the heart of mice for 4 weeks after TAC. Statistical significance of distributed data was analyzed by Log-rank (Mantel-Cox) test (C), by one-way (E-K) and two-way (D) ANOVA followed by Tukey's multiple comparisons test. **** P<0.0001, *** P<0.001, ** P<0.01, * P<0.05 versus vehicle group.

**Table 2:** Echocardiographic measurements in mice of each group

| **Groups** | **WT (n = 10)** | **Sham (n = 10)** | **TAC (n = 10)** | **TAC + ICG001 (n = 10)** |
|---|---|---|---|---|
| IVSd (mm) | 0.75 ± 0.08 | 0.76 ± 0.03 | 1.38 ± 0.16∗ | 0.79 ± 0.09# |
| IVSs (mm) | 1.09 ± 0.13 | 1.05 ± 0.09 | 0.93 ± 0.06∗ | 1.20 ± 0.10# |
| LVIDd (mm) | 3.66 ± 0.15 | 3.65 ± 0.14 | 4.19 ± 0.29∗ | 3.79 ± 0.22# |
| LVIDs (mm) | 2.41 ± 0.11 | 2.39 ± 0.09 | 3.26 ± 0.42∗ | 2.76 ± 0.24# |
| LVPWd (mm) | 0.76 ± 0.08 | 0.74 ± 0.04 | 0.97 ± 0.17∗ | 0.88 ± 0.13# |
| LVPWs (mm) | 1.15 ± 0.10 | 1.09 ± 0.12 | 1.30 ± 0.09∗ | 1.20 ± 0.16# |

| Groups | WT (n = 10) | Sham (n = 10) | TAC (n = 10) | TAC + ICG001 (n = 10) |
|---|---|---|---|---|
| LVEDV (μl) | 59.46 ± 7.20 | 58.08 ± 6.39 | 89.18 ±10.85∗ | 63.41±6.69# |
| LVESV (μl) | 21.18 ± 3.47 | 20.44 ± 2.01 | 46.69 ±6.48∗ | 29.59±5.52# |
| LV mass (corrected) (mg) | 85.84 ± 12.08 | 76.32 ± 9.21 | 99.78 ± 14.41∗ | 96.92 ± 18.58# |
| EF (%) | 64.44 ± 2.83 | 64.73± 1.71 | 45.78 ±5.72∗ | 57.17 ± 1.72# |
| FS (%) | 34.55 ± 2.07 | 34.58± 1.46 | 22.13±3.30∗ | 29.57 ± 1.06# |
| HR (beats/min) | 529.5 ±11.79 | 528.7± 11.99 | 535.1±10.26∗ | 531.1 ± 8.94# |

IVSd, interventricular septum depth at end diastole; IVSs, interventricular septum depth at end systole; LVIDd, left ventricular internal diameter at end diastole; LVIDs, left ventricular internal dimension at end systole; LVPWd, left ventricular posterior wall depth at end diastole; LVPWs, left ventricular posterior wall depth at end systole; LVEDV, left ventricular end diastolic volume; LVESV, left ventricular end systolic volume; LV mass (corrected); LVEF, left ventricular ejection fraction; LVFS, left ventricular fractional shortening; HR, heart rate; bpm, beats per minute. Statistical significance of distributed data was analyzed by one-way ANOVA followed by Tukey's multiple comparisons test. (n=10 in each group)

* $P < 0.05$ versus sham.

# $P < 0.05$ versus vehicle (untreated TAC mice).

**2. ICG001 attenuates cardiac hypertrophy in vivo and ameliorates pressure overload induced cardiac fibrosis**

To confirm whether ICG001 attenuates cardiac hypertrophy, the cardiac hypertrophy was observed in TAC mice compared with the sham mice as demonstrated by the increase of HW/BW ratio at the end of 4 weeks in TAC mice. The morphological changes and hematoxylin and eosin staining (HE) in heart section also revealed apparent change of hypertrophy in mice subjected to TAC, but ICG001-treated TAC mice markedly diminished the hypertrophic response to pressure overload. It was promising compared with ICG001-treated TAC mice which showed distinctly attenuated cardiac hypertrophy (Fig. 2A to C). These data indicate that the cardiac hypertrophy was attenuated after TAC and treated with ICG001. Intensive interstitial and perivascular fibrosis were regularly caused by prolonged pressure overload[22]. To confirm whether ICG001 attenuates cardiac fibrosis, the cardiac tissue sections were evaluated the fibrosis in each group by Masson's trichrome staining (MT). The increase of interstitial fibrosis in cardiac tissues was observed in the TAC mice which was not treated (Vehicle group), but this increase was alleviated in ICG001-treated TAC mice (Fig. 2D-E). As shown in Fig. 2F-H, the mRNA expression of several markers for cardiac fibrosis including connective tissue growth factor (*Ctgf*), fibronectin and collagen I were markedly reduced in the ICG001-treated TAC mice group compared with vehicle group. These data demonstrate that ICG001 ameliorates cardiac fibrosis induced by pressure overload.

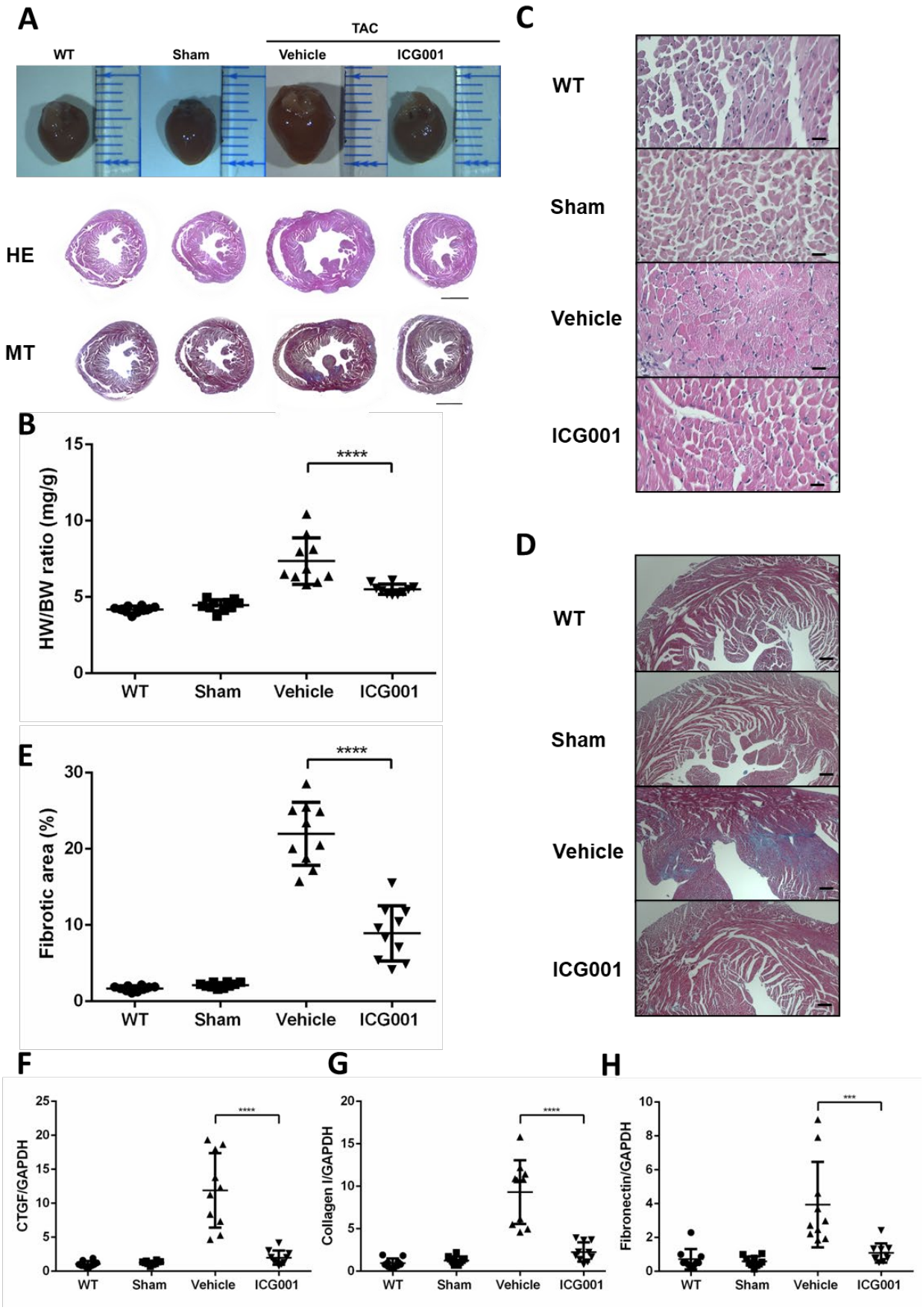
A
TAC
WT
Sham
Vehicle
ICG001
HE
MT
B
HW/BW ratio (mg/g)
****
WT
Sham
Vehicle
ICG001
C
WT
Sham
Vehicle
ICG001
D
WT
Sham
Vehicle
ICG001
E
Fibrotic area (%)
****
WT
Sham
Vehicle
ICG001
F
CTGF/GAPDH
****
G
Collagen I/GAPDH
****
H
Fibronectin/GAPDH
***

**Figure 2:** ICG001 attenuates cardiac hypertrophy in vivo and ameliorates pressure overload induced cardiac fibrosis.

(A) Representative images of heart size (upper panel), Hematoxylin and eosin (HE) staining (middle panel), and Masson & Trichrome (MT) staining (bottom panel) of cross sections of hearts of WT, sham, TAC mice, and ICG001 treated TAC mice at 4 weeks after TAC. Scale bar: 2 mm. (B) The heart weight to body weight (HW/BW) (n=10). (C) Histological analysis of heart sections was performed by HE staining. Scale bar: 200 μm. (D) MT staining. Scale bar: 200 μm. (E) Calculation of statistic for the results of fibrotic areas in the indicated group (n=10). (F-H) The relative connective tissue growth factor (CTGF), collagen I, and fibronectin levels of the LV in mice from the indicated groups (n=10). Statistical significance of distributed data was analyzed by one-way ANOVA followed by Tukey's multiple comparisons test. **** P<0.0001, *** P<0.001 versus vehicle group.

**3. ICG001 induces gene and protein expressions of cardiac hypertrophy and fibrosis after TAC**

After TAC induced cardiac hypertrophy and fibrosis and ICG001 ameliorated these effects, I next investigated whether ICG001 is associated with the role of KLF5 in the response of cardiac hypertrophy and fibrosis. Previous works showed that KLF5 promoted the cardiac hypertrophy and also regulated the expression of PPAR-α[30,31]. After TAC, the expression of KLF5 gene was upregulated in TAC mice and it was downregulated in mice treated ICG001. The results of KLF5 gene expression showed the significant difference between the ICG001-treated TAC mice and vehicle groups (Fig. 3E). Consistent with the KLF5 protein expression, ICG001 also significantly reduced the expression of KLF5 protein (Fig. 3A-B). Then, previous study reported that the

attenuation of the progression of HF and the improve of the survival rate by PPAR-α activator fenofibrate related with the repression of activation of redox-regulated transcription factors and inhibition of the inflammatory response in the left ventricle in rat model[32]. In this study, PPAR-α gene expression was decreased in TAC mice and significantly increased after treated with ICG001 (Fig. 3F). Similarly, protein expression of PPAR-α was significantly increased after TAC mice treated ICG001 (Fig. 3C). Because β-catenin is the intracellular mediator driving the transcription in Wnt signaling resulting in cardiac hypertrophy and fibrosis and fibrotic lesions after Ang II fusion were completely mitigated by ICG001[49]. To examine the effect of inhibition of Wnt/β-catenin signaling which play a role in mediating TAC-induced cardiac injury, the expression of β-catenin was observed. I found that TAC mice induced cardiac β-catenin activation. ICG001 significant suppressed β-catenin activation in protein expression, but not in gene expression (Fig. 3D and G). The results suggest that ICG001 inhibits cardiac β-catenin activation in Wnt/β-catenin signaling and might has an impact on protective effects against cardiac hypertrophy and fibrosis via KLF5 and PPAR-α.

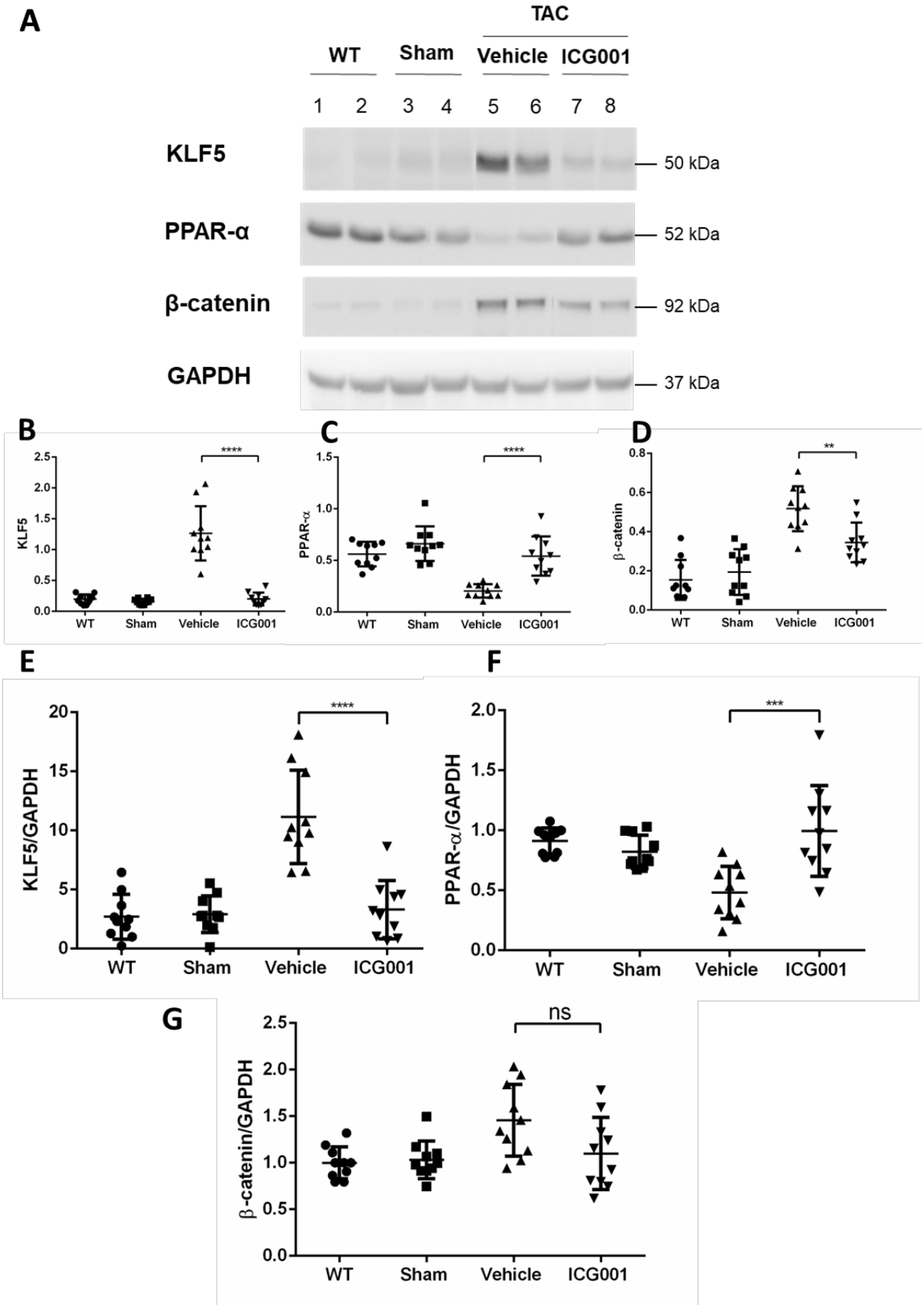
A
TAC
WT
Sham
Vehicle
ICG001
1 2 3 4 5 6 7 8
KLF5
PPAR-α
β-catenin
GAPDH
50 kDa
52 kDa
92 kDa
37 kDa
B
KLF5
****
C
PPAR-α
****
D
β-catenin
**
E
KLF5/GAPDH
****
F
PPAR-α/GAPDH
***
G
β-catenin/GAPDH
ns

**Figure 3:** ICG001 induces gene and protein expressions of cardiac hypertrophy and fibrosis after TAC.

(A) Western blot analyses showed protein expression of KLF5, PPAR-α, and β-catenin in heart of mice in various groups as indicated. (B-D) Quantitative data of protein levels of KLF5, PPAR-α, and β-catenin are shown in different groups as indicated (n=10). (E-H) real time polymerase chain reaction of KLF5, PPAR-α, and β-catenin in heart of mice in various groups as indicated (n=10). Statistical significance of distributed data was analyzed by one-way ANOVA followed by Tukey's multiple comparisons test. **** P<0.0001, *** P<0.001, ** P<0.01 versus vehicle group.

**4. ICG001 attenuates macrophage accumulation in cardiac tissues after TAC**

To test whether pressure-overload in the heart activates the accumulation of inflammatory cells and whether ICG001 influences to the accumulation of inflammatory cells in cardiac tissues, the hearts were analyzed by immunohistochemistry and flow cytometry analysis. The inflammatory cells have been studied in many previous works. They provided the information that inflammatory cells were associated with the development of cardiac hypertrophy. Recently, the data revealed the role of T cells and macrophages in cardiac hypertrophy and fibrosis[59,60,61]. The influence of pressure overload by TAC caused the distinct T cells accumulation and also caused the increase of macrophage infiltration in TAC mice[55]. Because of the inflammation resulted in the fibrosis in the TAC mice, therefore, I investigated the accumulation of T cells and macrophages in the heart after TAC. The immunohistochemical analysis of CD3 and CD68 in heart sections exhibited the T cells and macrophages infiltration in TAC mice. From immunohistochemistry studies, both of the T cells and macrophages were observed in cardiac tissues after TAC (Fig. 4A). T cells detected by CD3 did not significantly reduce in TAC mice treated with ICG001 (Fig. 4B). However, the

macrophages detected by CD68 were significantly reduced in ICG001-treated TAC mice (Fig. 4C). Furthermore, flow cytometry was performed to identify $CD45^{+}CD11b^{+}F4/80^{+}Ly6C^{+}CCR2^{+}$ cardiac macrophages with further investigate $CD45^{+}CD11b^{+}F4/80^{+}Ly6C^{+}CCR2^{-}$ macrophages. The results revealed that the significant reduction in levels of macrophage infiltrating in the tissue content of $CD45^{+}CD11b^{+}F4/80^{+}Ly6C^{+}CCR2^{+}$, and $CD45^{+}CD11b^{+}F4/80^{+}Ly6C^{+}CCR2^{-}$ macrophages was observed in ICG001-treated TAC mice (Fig. 4D-E). ICG001 reduced both tissue resident cardiac macrophages $CCR2^{+}$ and $CCR2^{-}$ after TAC. Next, treatment of mice with ICG001 also led to a marked reduction in transcripts that encode inflammatory mediators including interleukin 4 (*Il4*), interleukin 10 (*Il10*), transforming growth factor beta 1 (*Tgfb1*), tumor necrosis factor alpha (*Tnfa*), and chemokine (C-C motif) ligand 2 (*Ccl2*) in heart at 4 weeks after TAC (Fig. 4F-J). These results demonstrate that ICG001 might regulate the inflammation in heart tissues through influencing macrophages and reduce the macrophage accumulation after TAC.

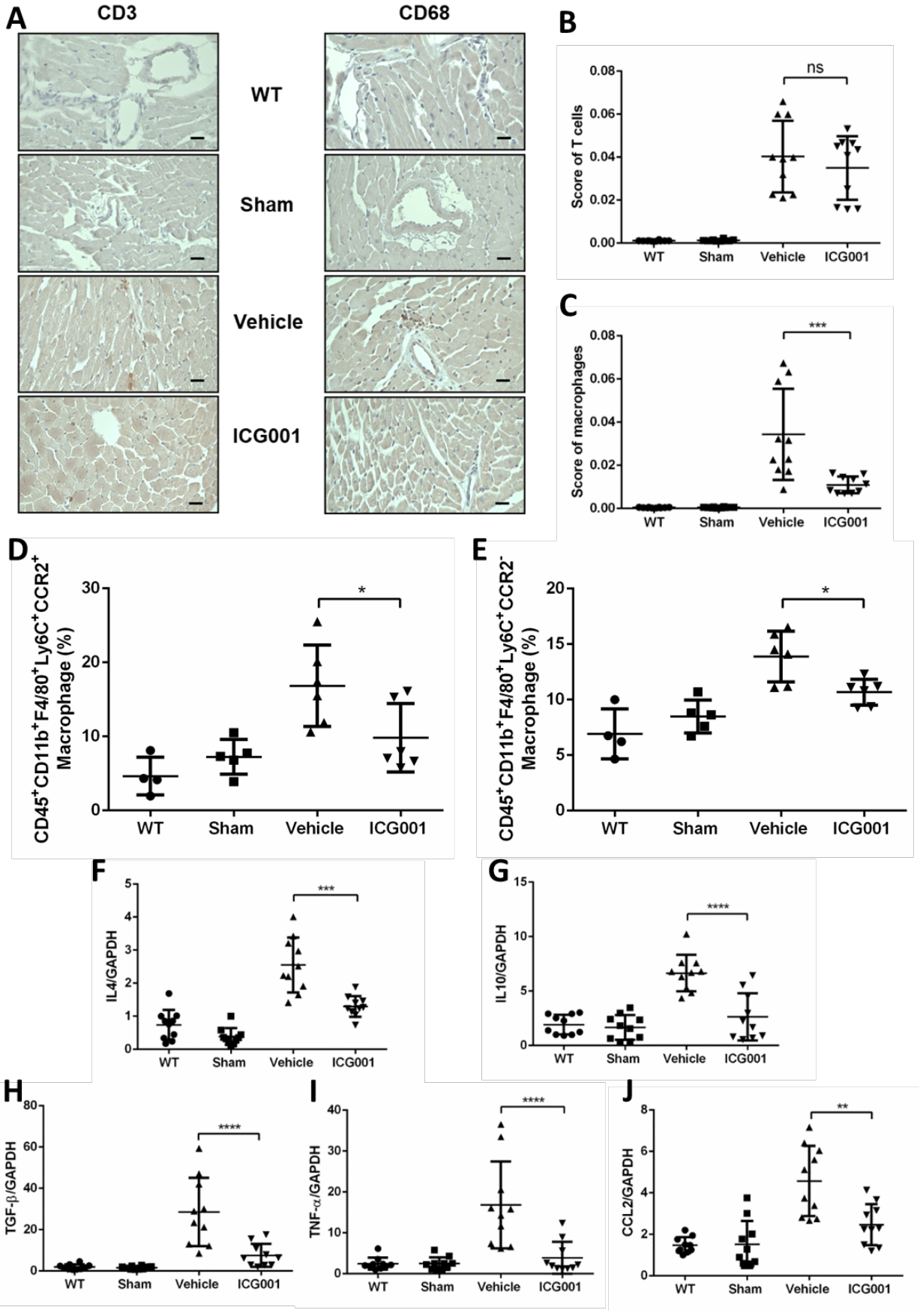
A
CD3
CD68
WT
Sham
Vehicle
ICG001
B
Score of T cells
ns
C
Score of macrophages
***
D
CD45+CD11b+F4/80+Ly6C+CCR2+ Macrophage (%)
*
E
CD45+CD11b+F4/80+Ly6C+CCR2- Macrophage (%)
*
F
IL4/GAPDH
***
G
IL10/GAPDH
****
H
TGF-β/GAPDH
****
I
TNF-α/GAPDH
****
J
CCL2/GAPDH
**
WT
Sham
Vehicle
ICG001

**Figure 4:** ICG001 attenuates macrophage accumulation in cardiac tissues after TAC.
(A) Immunohistochemical analysis of CD3 and CD68 in heart sections (n=10, Scale bar=200 μm). (B-C) Score of T cells and macrophages in immunohistochemical analysis calculated by Image-J. (D-E) Flow cytometry analysis of macrophages $CD45^{+}CD11b^{+}F4/80^{+}Ly6C^{+}CCR2^{+}$, and $CD45^{+}CD11b^{+}F4/80^{+}Ly6C^{+}CCR2^{-}$ macrophages in mice at 4 weeks after TAC (n=4-6). (F-J) real time polymerase chain reaction of *Il4*, *Il10*, *Tgfb1*, *Tnfa*, and *Ccl2* in heart at 4 weeks after TAC. Statistical significance of distributed data was analyzed by one-way ANOVA followed by Tukey's multiple comparisons test. **** P<0.0001, *** P<0.001, ** P<0.01, * P<0.05 versus vehicle group.

**5. ICG001 mediated the substrate metabolism and metabolic alteration in TAC mice**

Activating PPAR-α transcription showed the improve of the function and energetics of the heart[39] and the evaluation of metabolic changes in hypertrophic and HF in ICG001-treated mice remain unrevealed; hence, I investigated the effect of ICG001 on metabolic alteration in the heart by mass spectrometry. Here, I investigated the impact of hypertrophy and HF by pressure overload on metabolic alteration. Substrate metabolism was determined from heart of WT, sham, vehicle and ICG001-treated TAC mice. In glycolysis pathway, the increase of levels of glucose-1-phosphate (G1P) and glucose-6-phosphate (G6P) was found in TAC mice which was higher than in sham; however, both levels decreased in ICG001-treated TAC mice but were not statistically significant compared with TAC mice. Meanwhile, glycerol-3-phosphate (G3P) was increased in TAC mice but was reduced in ICG001-treated TAC mice. Compared with sham and ICG001-treated TAC mice, TAC mice had increased levels of pyruvate, alanine, and lactate in the glycolysis pathway and demonstrated minor changes in TCA cycle intermediates such as citrate, fumarate, and malate after TAC. Moreover, aspartate was increased after TAC, but it was

significantly decreased in ICG001-treated TAC mice. Regarding methionine and cysteine metabolisms, methionine was increased after TAC and it was reduced in TAC mice treated with ICG001. Moreover, the indices of oxidative stress were assessed according to the ratio of reduced (GSH) and oxidized glutathione (GSSG). Compared with that in sham, the ratio of GSH/GSSG was slightly decreased in ICG001-treated TAC mice, but further decreased in TAC mice (Fig. 5A, B). Taken together, ICG001 may mediate the substrates in the glycolysis pathway and the distinct alteration of oxidative stress during cardiac hypertrophy and HF. In addition, the metabolites and amino acids including isoleucine, leucine, lysine, valine, phenylalanine, serine, tryptophan, and tyrosine increased in TAC mice, but they were significantly attenuated in ICG001-treated TAC mice (Fig. 5C).

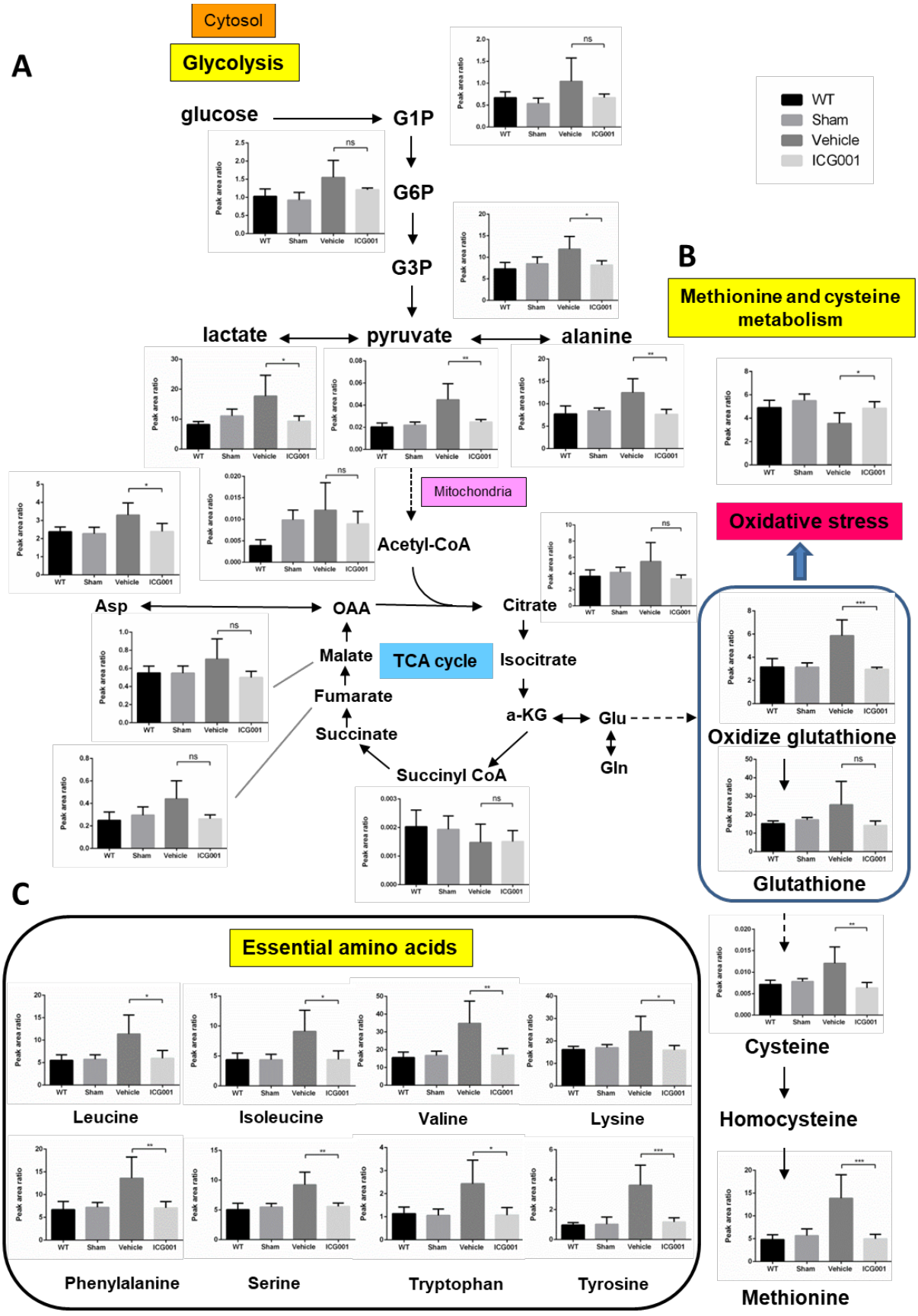
A
Cytosol
Glycolysis
glucose
G1P
G6P
G3P
lactate
pyruvate
alanine
Mitochondria
Acetyl-CoA
Asp
OAA
Citrate
Malate
TCA cycle
Isocitrate
Fumarate
a-KG
Glu
Succinate
Succinyl CoA
Gln
B
Methionine and cysteine metabolism
Oxidative stress
Oxidize glutathione
Glutathione
Cysteine
Homocysteine
Methionine
C
Essential amino acids
Leucine
Isoleucine
Valine
Lysine
Phenylalanine
Serine
Tryptophan
Tyrosine
WT
Sham
Vehicle
ICG001
Peak area ratio

**Figure 5:** Substrate metabolism and metabolic alteration in ICG001-treated TAC mice.

Data are normalized to internal control when unit is indicated by area ratio. (A) The metabolic profiling in glycolysis pathway and TCA cycle of heart tissues from mice in the indicated group (n=4-5). (B) The metabolic profiling in methionine and cysteine showed the oxidative stress calculated from the ratio of reduced and oxidized glutathione (GSH/GSSG) (n=4-5). (C) The levels of essential amino acids in heart tissues from mice in the indicated group (n=4-5). Statistical significance of distributed data was analyzed by one-way ANOVA followed by Tukey's multiple comparisons test. *** $P<0.001$, ** $P<0.01$, * $P<0.05$ versus vehicle group. G1P= Glucose-1-phosphate, G6P= Glucose-6-phosphate, G3P= Glycerol-3-phosphate, α-KG= Alpha-ketoglutarate, Glu= Glutamic acid, Gln= Glutamine, OAA= Oxaloacetic acid, Asp= Aspartic acid.

# CHAPTER V

# DISCUSSION

These findings in this study disclose various aspects identifying that ICG001 attenuate the cardiac function and prevent HF after pressure overload. TAC mouse model as reflected in the potential method to induce pressure overload by using 27G TAC displayed cardiac dysfunction or HF after TAC at 4 weeks. In order to identify the role of ICG001, I used the higher dose of ICG001 (50 mg/kg/day) as suggested that to certify better coverage for extendible period of time because of a limited half-life of ICG001 in rodents[52]. In this study, ICG001 increased survival of mice with HF suggesting that ICG001 influences to the process of cardiac hypertrophy driving through cardiac dysfunction or HF. TAC caused cardiac dysfunction marked by the increase of LVIDs and LVIDd while the EF was decreased. ICG001 demonstrated the amelioration of EF after TAC and prevented the increase of LVIDs, LVIDd, and LV mass. Therefore, ICG001 increased the survival of TAC mice and maintained cardiac function as judged by improvement of EF. Previously, ICG001 improved contractile function in chronically infarcted rat myocardium by significant improvement of EF[52]. Moreover, ICG001 showed the decrease of LVIDs and LVIDd and also prevented the reduction of EF[53]. Conversely, the present study showed that ICG001 prevents HF by itself for the first time.

Generally, Wnt signaling in adult tissues is silent, but Wnt/β-catenin is activated after injury or disorder[58,62-64,65,66]. TAC has been associated with the upregulation of several Wnt ligands in the cardiac tissue and activation of β-catenin[53]. The representative micrographs of the immunohistochemical staining for β-catenin in heart showed that the β-catenin predominantly localized in the cytoplasma of cardiomyocytes in mice after TAC[53]. Here, TAC mice showed the activation of Wnt signaling gene expression including Wnt1 and Wnt3a. Similarly, TAC induced

the upregulation of canonical Wnt signaling in mice and increased Wnt/β-catenin signaling in cardiac fibroblasts[53,67]. β-catenin acted as a transcription factor for several target genes related with hypertrophy[64]. β-catenin is the intracellular mediator driving the transcription in Wnt signaling resulting in cardiac hypertrophy and fibrosis and ICG001 completely mitigated fibrotic lesions after Ang II fusion[49]. The hypertrophic growth expressed in cardiomyocytes in vitro and in vivo was induced by β-catenin and transcriptional activating activity of β-catenin is indispensable for the hypertrophic response to physiologically relevant stimuli[68]. In this study, I also found that expression of the β-catenin mRNA and protein was increased in TAC mice and was decreased in ICG001-treated TAC mice. The inhibition of β-catenin by ICG001 was also shown by the TOPFLASH reporter system suggesting that ICG001 inhibited TCF/β-catenin transcription in a CBP-dependent fashion[62,69]. Therefore, ICG001 prevented HF likely by inhibition of β-catenin activating the transcription in Wnt signaling. In response to cardiac overload, changes in the gene transcription program were associated with HF marker including BNP and β-MHC[70]. Upregulation of BNP and β-MHC has been reported in cardiac hypertrophy and HF[5,71,72]. As expected, gene expression of BNP and β-MHC was increased in TAC mice and reduced in TAC mice treated with ICG001. Thus, the downregulation of HF markers also supports the prevention of HF by ICG001.

Next, I observed whether ICG001 attenuated the cardiac hypertrophy in mice subjected to TAC. The cardiac cross sections and HE staining revealed apparent hypertrophic change TAC mice, but ICG001 prevented the hypertrophic response from pressure overload in TAC mice. From this experiment, the prevention of the HW/BW ratio increase was also markedly exhibited in the ICG001-treated TAC mice. The reduction of cardiac hypertrophy in TAC mice by ICG001 correlated with the decrease of HW/BW ratio in ICG001-treated TAC mice. These findings were supported by the previous assessment of morphology and immunostaining of heart sections which

cardiomyocyte hypertrophy was caused by TAC, but this change was inhibited by ICG001 or losartan[53]. To understand the target cells of ICG001 in the TAC model, the experiment in vitro should be unveiled. Here, the effect of ICG001 on the cell was not assessed by in vitro experiment. As shown in previous work, ICG001 completely abolished the hypertrophic response of primary cardiomyocytes to Ang II stimulation[49]. I found that ICG001 reduced the expression of β-catenin which was up-regulated in both cardiomyocyte and interstitial fibroblasts[49]. Therefore, I also think that ICG001, β-catenin inhibitor, might perform the effect to the cardiac hypertrophy and fibroblast which hypothesize as the target cells in TAC mice. From my result at the present, I cannot point out the potential direct target of ICG001. However, to confirm the direct target cell of ICG001 in TAC model will be planned to investigate in the future. In addition, I also found that the evaluation of fibrosis by MT staining of heart sections demonstrated the increase of fibrosis in TAC mice, but ICG001 relieved TAC mice from infiltration of fibrosis in cardiac interstitium. Consistent with previous works, ICG001 was shown to prevent fibrosis and improved survival rate of animal in various pathologies such as idiopathic pulmonary fibrosis[62]. ICG001 completely mitigated the fibrotic lesions in the interstitial compartment of the heart in Ang II model[49]. ICG001 also ameliorated cardiac fibrosis and renal fibrotic lesions in TAC mice[53]. Because cardiac fibrosis is a hallmark for pathological foundation of cardiac dysfunction and occur during the development of cardiac remodeling[9], the decrease of fibrosis by ICG001 may be related to KLF5 expression in cardiac fibroblast. KLF5 controlled cardiac fibroblasts which is the core of proteins that cause cardiac fibrosis[12]. Furthermore, TGF-β was directly controlled by KLF5 and played a role in the progression of fibrosis in various chronic inflammatory conditions[73]. Inhibition of TGF-β mediated upregulation of α-SMA and collagen I by ICG001 has been shown in mouse fibroblasts and human hepatic stellate cells (HSCs)[74,75]. In this study, I also found the ICG001 has an effect on the

expression of KLF5 and TGF-β. TGF-β was a downstream of KLF5 and a critical initiator in tissue fibrosis by controlling the production of the extracellular matrix (ECM) components such as collagen and fibronectin[15,76]. Here, I am hypothesizing that inhibition of β-catenin by ICG001 can prevent the cardiac fibroblast from producing fibrosis via the regulation of KLF5 and TGF-β. Thus, cardiac fibroblasts are likely to be one of the target cells. In the future study, I will experimentally support that ICG001 targets cardiac fibroblasts and show the precise effect of ICG001 on cardiac fibroblasts. Moreover, to compare the occurrence between cardiac hypertrophy and fibrosis in the consequence of TAC, previous work showed that the increase of cardiomyocyte size and volume by cellular dimension was found at every time point post-TAC and TAC mice was not found a significant increase in collagen volume fraction or myocardial ECV by CMR at 2 weeks, 4 weeks, or 7 weeks after TAC[77]. Therefore, from the consequence of TAC, I think that TAC causes the cardiac hypertrophy before fibrosis. To confirm the decrease of fibrosis by ICG001, fibrosis markers were checked. Here, ICG001 reduced the expression of fibrosis markers including Ctgf, fibronectin, and collagen I. The expression of the fibrosis markers correlated with the size of fibrosis in cardiac tissues. This result is consistent with previous works which presented the photomicrograph of the reduced β-MHC and fibronectin protein expressions in the heart of TAC mice treated with ICG001 or losartan[53]. In addition, treatment with ICG001 in TAC mice restrained TAC-induced expression of fibronectin and collagen I in the heart[53]. Accordingly, the reduction of fibrosis in TAC mice by ICG001 prevented pressure overload-induced HF.

KLF5 was reported to control cardiac fibroblasts, which play an important role in the myocardial adaptive response to pressure overload, and the upregulation of KLF5 expression was induced by TAC[16,17]. Here, I found that the gene and protein expressions of KLF5 were upregulated after TAC. Importantly, I found that ICG001 diminished the increase of KLF5

expression in TAC mice subjected to pressure-overload. The decrease of KLF5 expression in ICG001-treated TAC mice may have reduced the fibrosis in the heart tissue because fibrosis is one of the downstream effects of KLF5 upregulation[15,78,79]. The inhibition of β-catenin by ICG001 influenced to the regulation of KLF5. This study raises question whether β-catenin and KLF5 function independently or in tandem in the ICG001-treated TAC mice and this question will be needed to clarify in the future. Moreover, KLF5 controlled macrophage polarity in chronic inflammatory diseases[80]. Considering that *Klf5* haploinsufficiency decreases M1 macrophage accumulation[18], I tested whether TAC-induced pressure overload in the mice activated the accumulation of inflammatory cells in cardiac tissues. Both the T cell and macrophage infiltrations were observed in the cardiac tissues after TAC. Importantly, ICG001 suppressed the infiltration of macrophages but ICG001 did not influence T cells. Previously, inflammatory cells were associated with the progression of cardiac hypertrophy[59,60]. Lately, the data revealed that the accumulation of T cells and macrophages in the heart was found during cardiac hypertrophy and fibrosis[59,60,61,81,82]. TAC caused the distinct accumulation of T cells and also caused the increase of macrophage infiltration in the heart[27,55,83]. Here, ICG001 had an impact on reducing the accumulation of macrophages. I also confirmed the accumulation of T cells and macrophages by flow cytometry analysis. The results revealed that the macrophage accumulation in TAC mice was reduced by ICG001 treatment, but ICG001 did not reduce T cell accumulation after TAC. Previous studies were revealed the trend towards the expansion of cardiac $F4/80^+$ macrophages and the increase in $CD11b^+$, $Ly6G^-$, $F4/80^+$ macrophage accumulation after TAC[84]. Recent studies exhibited that the numbers of infiltration of $CCR2^+$ monocytes and the proliferation of resident of cardiac macrophages were increased after Ang-II infusion[85]. $CCR2^+$ macrophages and $CCR2^-$ tissue resident cardiac macrophages were increased in the heart one week after TAC. Moreover,

$Ly6C^{hi}CCR2^{+}$ monocytes were increased one and four weeks after TAC[56]. In this study, ICG001 reduced both $CD45^{+}CD11b^{+}F4/80^{+}Ly6C^{+}CCR2^{+}$ and $CD45^{+}CD11b^{+}F4/80^{+}Ly6C^{+}CCR2^{-}$ macrophages after TAC. Moreover, I found that ICG001-treated TAC mice exhibited a marked reduction in transcripts that encode inflammatory mediators including *Il4*, *Il10*, *Tgfb1*, *Tnfa*, and *Ccl2* in heart after TAC. CCL2 binds to CCR2 expressed on monocytes and promotes the recruitment of monocyte, resulting in increasing the number of macrophages in the tissue[56]. The monocytes/macrophages were recruited from bone marrow by the pathway of CCR2/CCL2 and conduced to heart inflammation in response to HF[85]. Therefore, I speculated that ICG001 might have inhibitory effect on CCR2 monocytes recruitment from bone marrow during pressure overload. Then, the macrophage expansion during pressure overload was found to correlate with overexpression of *Tnfa*, *Tgfb1*, and *Ccl2*[56]. CCL2 is chemotactic to monocytes[18]. ICG001 influenced to the infiltration of macrophage and affected to Wnt-dependent by HSCs causing the decrease of hepatic inflammation[74,75]. In-vivo, ICG-001 showed the reduction of collagen accumulation and HSC activation and also inhibited macrophage infiltration, intrahepatic inflammation and angiogenesis[60,75]. Hence, CCL2 reduction by ICG001 may have minimized the recruitment of monocytes, resulting in macrophage decrease in the heart. Reducing the expression of inflammatory cytokines such as IL-4, IL-10, and TNFα inhibits the pressure overload-induced cardiac dysfunction or attenuation of cardiac hypertrophy and fibrosis in mice[29,86];therefore, the reduction of such cytokines by ICG001 injection may also contribute to HF prevention. In addition, fibroblasts activated by macrophages produce ECM proteins[87]. I am hypothesizing that the ICG001 may regulate the process of repair that involving in the fundamental role of inflammatory cells in the progression of pathological hypertrophy and cardiac fibrosis after pressure overload. Thus, reduction of macrophage accumulation by ICG001 may also contribute to fibrosis attenuation.

Time course studies previously revealed that the increase of cardiac macrophages was increased to the peak at 7 days after TAC and it was reduced to baseline after 2 weeks and then was increased modestly at 4 weeks after TAC[88]. Considering that the cardiac resident macrophage proliferation occurred within the first week after pressure overload, reducing macrophage proliferation in the early phase may be important for cardiac repair and HF prevention. The previous study showed the use of ICG001 for the treatment of HF[53]. Since the prevention in the early stage is important more than the treatment in the late stage[89], in this study, ICG001 was injected into the TAC mice for 10 days before the onset of HF. ICG001 could reduce the macrophage accumulation after TAC. Reduction of macrophages by ICG001 resulted in preventing HF in TAC mice. However, timing of the injection of ICG001 to prevent macrophages accumulation may be crucial for prevention of HF in TAC mice. This finding suggested that ICG001 may prevent further macrophage proliferation in the early phase and has a potential effect to prevent macrophage accumulation in TAC mice. A new finding from this study suggests that starting treatment with ICG001 prior to the onset of HF can improve the survival rate of TAC mice. The timing of ICG001 injection in this study is suitable for the prevention of HF in TAC mice. Because macrophages are known to be the major contributors of inflammatory and fibrotic processes in HF[90] and ICG001-treated TAC mice show the reduction of fibrosis, macrophage accumulation, and the expression of inflammatory cytokines, the reduction of macrophage accumulation by ICG001 may also contribute to fibrosis attenuation.

Next, previous works showed that KLF5 not only promoted the cardiac hypertrophy but also regulated the expression of PPAR-α[30,31]. It was reported that PPAR-α levels were reduced after pressure overload[39]. The activation of PPAR-α during HF improved the function of myocardial and energetics[39]. Here, I found that gene and protein expressions of PPAR-α were

decreased in TAC mice. Importantly, I found that the expression of PPAR-α was increased in ICG001-treated TAC mice. Consistent with previous reports[38,39,91], gene and protein expressions of PPAR-α were reduced after TAC model. The level of complexity in the PPAR-α regulatory mechanism comes from its ability to interact with various partners and the regulatory mechanisms of PPAR-α are greatly complex in heart disease[92]. This study only showed the change of expression of PPAR-α to compare between WT, sham, TAC mice and ICG001-treated TAC mice. The potential molecular mechanism of regulation of PPAR-α and the relationship between canonical Wnt/beta-catenin pathway and PPAR-α activity is unclear. In the future, the factors upstream of PPAR-α in HF prevention should be identified for understanding the relation between PPAR-α and β-catenin in order to explain in mechanism of prevention of HF by ICG001.

Cardiac hypertrophy and HF were involved in abnormality or impairment in the regulation of a metabolism and the state of chronic energy deficiency[93]. PPAR-α played a critical role in metabolic regulatory processes, particularly in heart muscle[39]. The heart produced the energy by switching from fatty acid oxidation to glucose oxidation in failing heart[43,45]. PPAR-α is deactivated at several levels during cardiomyocyte hypertrophic growth, leading to reduced capacity for myocardial lipid metabolism[41]. In hypertrophic heart, the expression of PPAR-α and its activity were decreased, leading to the reduction in the capacity for FAO and increased rate of glucose oxidation[94]. Activating PPAR-α transcription reportedly improves the function and energetics of the heart[39], and the evaluation of metabolic changes in hypertrophic and HF in ICG001-treated TAC mice remain unrevealed; hence, as I found that ICG001 elevated the expression of PPAR-α, I evaluated the effect of ICG001 on metabolic alteration in the heart. In the glycolysis pathway, ICG001 did not influence G1P and G6P but influenced G3P, which is a metabolite connecting glycolysis, lipogenesis, and oxidative stress after TAC. The ICG001 also reduced the pyruvate,

alanine, and lactate levels. From the previous study, alanine and lactate levels were increased in TAC mice but not in sham, suggesting to decrease the flux of pyruvate into the TCA cycle with diversion to lactate[95]. Metabolic analysis also revealed that the aspartate levels significantly increased after 1, 2, or 4 weeks in TAC mice, with correlation with cardiac hypertrophy[96,97]. The metabolic analysis in this study showed that alanine, lactate, and aspartate accumulated in TAC mice but this accumulation was prevented by ICG001 treatment. ICG001 might control the metabolism in TAC mice by retarding the accumulation of lactate, alanine, and aspartate, thereby preventing cardiac hypertrophy and HF. As shown in previous study, up-regulation of the cardiac lipid metabolism and overload of toxic lipid also caused the onset of HF[98]. In this study, I focused on the glycolysis pathway; however, the change in the lipid pathway will be investigated in the future. Next, the development and progression of clinical and experimental HF associated with oxidative stress[99]. In the methionine and cysteine metabolisms, the oxidative stress indicated by the GSH/GSSG ratio[100] was significantly higher in the ICG001-treated TAC mice than in the TAC mice. Because a higher ratio of GSH/GSSG means the reduction of oxidative stress and a lower ratio of GSH/GSSG means the increase of oxidative stress[101], the oxidative stress was increased after TAC but was subsequently reduced by ICG001. Thus, ICG001 may reduce or mediate the distinct alteration of oxidative stress during myocardial hypertrophy and HF. Furthermore, HF also increased the level of essential amino acids[102]. One of the most noticeable metabolic changes was found in branched-chain amino acid (BCAA) metabolism. For mammals, BCAAs such as leucine, isoleucine, and valine act as essential nutrient signal molecules that control cellular metabolism and growth[103]. Metabolic profiling demonstrated that amino acids including isoleucine, leucine, lysine, valine, phenylalanine, serine, tryptophan, and tyrosine were increased in TAC mice but significantly decreased in ICG001-treated TAC mice. Reducing the

cardiac intratissue concentration of BCAA in TAC mice by increasing the BCAA catabolism preserves cardiac function and structure[104]; thus, stimulating BCAA catabolism via PPAR-α upregulation may be one of the mechanisms that ICG001 protects the heart from HF. The previous work showed the switch of fatty acid oxidation towards glucose oxidation and altered amino acid metabolism as well as elevation of oxidative stress in HF[105]. The new finding in the metabolic alteration suggests that decreasing lactate accumulation in the glycolysis pathway and reducing oxidative stress may be a new target to prevent HF. The results of metabolic alteration in ICG001-treated TAC mice increase the understanding of the role of ICG001 in preventing HF. However, this study only evaluated and reported the metabolic changes in hypertrophic and failing hearts of TAC mice in comparison with those in sham and ICG001-treated TAC mice. The further understanding of the metabolic alteration by ICG001 in preventing and improving cardiac hypertrophy and HF is required in the future. Here limitations of this study are as follows: analysis of limited immune factors and only two time points, namely, before TAC and 4 weeks after TAC. Future studies are planned to broaden both the immune factors and the time points of analysis after TAC. Although there are advances in the molecular understanding of ICG001 for HF, it remains not to be the concrete in the clinical trial. Hence, the identification of ICG001 with therapeutic potential in the clinical trial of HF is an area of need in the future. Moreover, the adverse effects due to the long-term administration of ICG001 need to be further investigated in the future. The experiment will be planned to test the adverse effects of using ICG001 for long-term in mice and also evaluate the effects of ICG-001 treatment for long-term in cells. In this study, ICG001 prevented the heart from developing hypertrophy and dysfunction by reducing the fibrosis and macrophage accumulation and induced change in substrate metabolism after pressure overload (Fig. 6). In conclusion, ICG001 can prevent HF from cardiac hypertrophy and fibrosis

due to pressure overload by inhibition of Wnt/β-catenin signaling involved in reduction of KLF5 expression and macrophage recruitment. In addition, this study reveals the novel mechanism associated with the reduction of oxidative stress via metabolic alteration that can improve the knowledge of ICG001 in preventing HF.

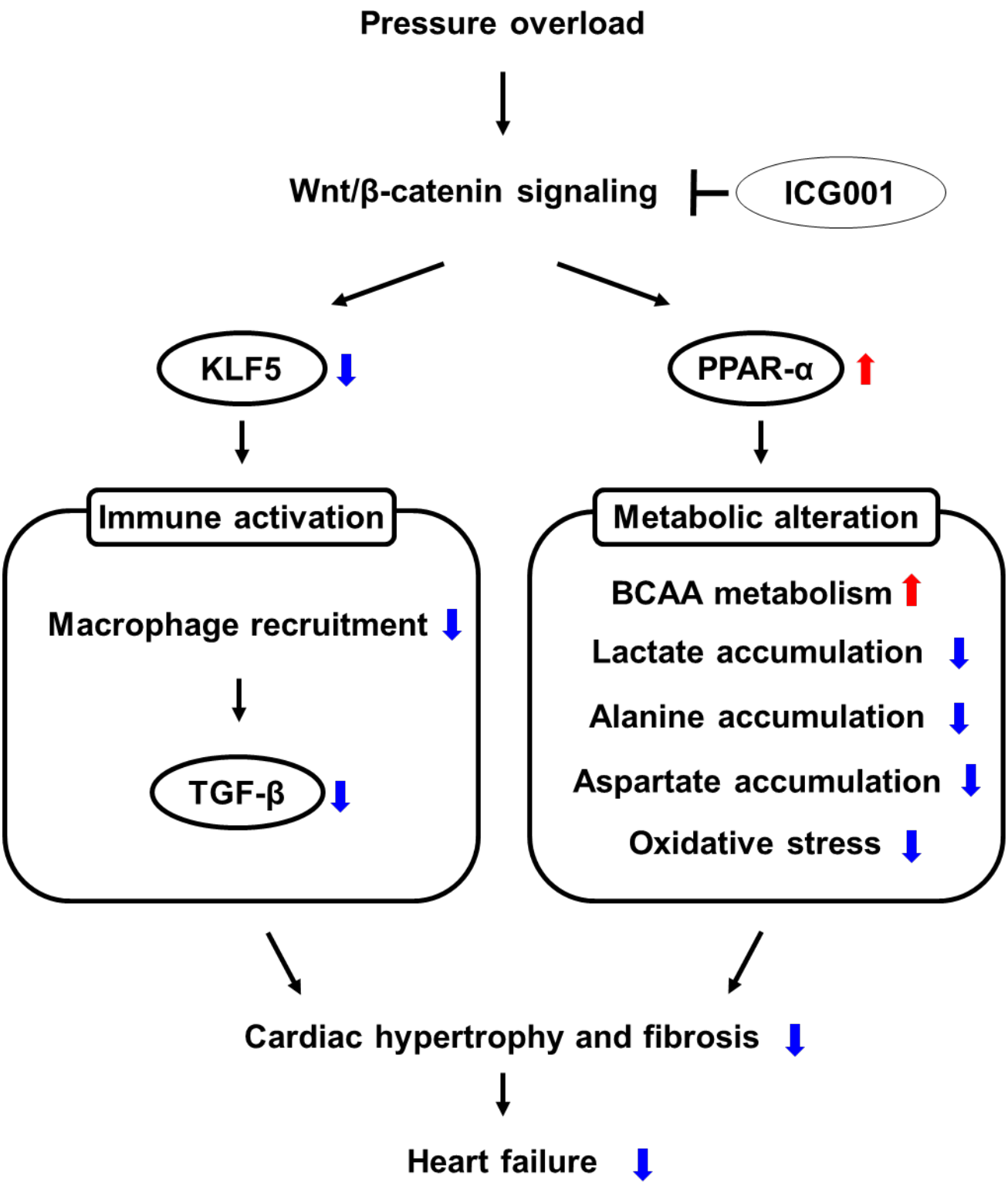
Pressure overload
Wnt/β-catenin signaling
ICG001
KLF5
PPAR-α
Immune activation
Macrophage recruitment
TGF-β
Metabolic alteration
BCAA metabolism
Lactate accumulation
Alanine accumulation
Aspartate accumulation
Oxidative stress
Cardiac hypertrophy and fibrosis
Heart failure

**Figure 6:** Summary of the proposed pathways of the role of ICG001 to attenuate cardiac hypertrophy and ameliorate pressure overload induced cardiac fibrosis.

This study suggests that pressure overload could lead to heart failure through 2 pathways, both of which are resulted from alteration of Wnt/β-catenin signaling. The first involved immune activation mediated by KLF5 activation, while the second is associated with PPAR-α downregulation that will cause metabolic alteration. In the presence of ICG001, inhibition of Wnt/β-catenin signaling will lead to reduce KLF5 expression which linked to the reduction of macrophage recruitment and TGF-β expression. Moreover, ICG001 seems to reduce oxidative stress via metabolic alteration due to PPAR-α upregulation. Both pathways ameliorated cardiac hypertrophy and fibrosis and ultimately prevented HF.

# CHAPTER VI

# CONCLUSION

In this study, ICG001 is a potential drug that may prevent cardiac hypertrophy and fibrosis through regulating KLF5, immune activation, and the Wnt/β-catenin signaling pathway and also inducing the change in substrate metabolism after pressure overload.

## REFERENCES

1 Benjamin, E. J., Blaha, M. J., Chiuve, S. E., Cushman, M., Das, S. R., Deo, R., De Ferranti, S. D., Floyd, J., Fornage, M. & Gillespie, C. Heart disease and stroke statistics—2017 update. (2017).

2 Shimizu, I. & Minamino, T. Physiological and pathological cardiac hypertrophy. *Journal of molecular and cellular cardiology* **97**, 245-262 (2016).

3 deAlmeida, A. C., van Oort, R. J. & Wehrens, X. H. Transverse aortic constriction in mice. *JoVE (Journal of Visualized Experiments)*, e1729 (2010).

4 Bosch, L., de Haan, J. J., Bastemeijer, M., van der Burg, J., van der Worp, E., Wesseling, M., Viola, M., Odille, C., El Azzouzi, H. & Pasterkamp, G. The transverse aortic constriction heart failure animal model: a systematic review and meta-analysis. *Heart Failure Reviews* (2020).

5 Richards, D. A., Aronovitz, M. J., Calamaras, T. D., Tam, K., Martin, G. L., Liu, P., Bowditch, H. K., Zhang, P., Huggins, G. S. & Blanton, R. M. Distinct phenotypes induced by three degrees of transverse aortic constriction in mice. *Scientific Reports* **9**, 1-15 (2019).

6 Zi, M., Stafford, N., Prehar, S., Baudoin, F., Oceandy, D., Wang, X., Bui, T., Shaheen, M., Neyses, L. & Cartwright, E. J. Cardiac hypertrophy or failure?-A systematic evaluation of the transverse aortic constriction model in C57BL/6NTac and C57BL/6J substrains. *Current Research in Physiology* **1**, 1-10 (2019).

7 Creemers, E. E. & Pinto, Y. M. Molecular mechanisms that control interstitial fibrosis in the pressure-overloaded heart. *Cardiovascular research* **89**, 265-272 (2011).

8 Travers, J. G., Kamal, F. A., Robbins, J., Yutzey, K. E. & Blaxall, B. C. Cardiac fibrosis: the fibroblast awakens. *Circulation research* **118**, 1021-1040 (2016).

9 Kong, P., Christia, P. & Frangogiannis, N. G. The pathogenesis of cardiac fibrosis. *Cellular and molecular life sciences* **71**, 549-574 (2014).

10 Fan, D., Takawale, A., Lee, J. & Kassiri, Z. Cardiac fibroblasts, fibrosis and extracellular matrix remodeling in heart disease. *Fibrogenesis & tissue repair* **5**, 15 (2012).

11 Ivey, M. J. & Tallquist, M. D. Defining the cardiac fibroblast. *Circulation Journal*, CJ-16-1003 (2016).

12 Ceccato, T. L., Starbuck, R. B., Hall, J. K., Walker, C. J., Brown, T. E., Killgore, J. P., Anseth, K. S. & Leinwand, L. A. Defining the Cardiac Fibroblast Secretome in a Fibrotic Microenvironment. *Journal of the American Heart Association* **9**, e017025 (2020).

13 Nagai, R., Suzuki, T., Aizawa, K., Shindo, T. & Manabe, I. Significance of the transcription factor KLF5 in cardiovascular remodeling. *Journal of Thrombosis and Haemostasis* **3**, 1569-1576 (2005).

14 Salmon, M. in *Gene Expression and Phenotypic Traits* (IntechOpen, 2020).

15 Shindo, T., Manabe, I., Fukushima, Y., Tobe, K., Aizawa, K., Miyamoto, S., Kawai-Kowase, K., Moriyama, N., Imai, Y. & Kawakami, H. Krüppel-like zinc-finger transcription factor KLF5/BTEB2 is a target for angiotensin II signaling and an essential regulator of cardiovascular remodeling. *Nature medicine* **8**, 856-863 (2002).

16 Takeda, N., Manabe, I., Uchino, Y., Eguchi, K., Matsumoto, S., Nishimura, S., Shindo, T., Sano, M., Otsu, K. & Snider, P. Cardiac fibroblasts are essential for the adaptive response of the murine heart to pressure overload. *The Journal of clinical investigation* **120**, 254-265 (2010).

17 Fujiu, K., Shibata, M., Nakayama, Y., Ogata, F., Matsumoto, S., Noshita, K., Iwami, S., Nakae, S., Komuro, I. & Nagai, R. A heart–brain–kidney network controls adaptation to cardiac stress through tissue macrophage activation. *Nature medicine* **23**, 611-622 (2017).

18 Fujiu, K., Manabe, I. & Nagai, R. Renal collecting duct epithelial cells regulate inflammation in tubulointerstitial damage in mice. *The Journal of clinical investigation* **121** (2011).

19 Taqueti, V. R., Mitchell, R. N. & Lichtman, A. H. Protecting the pump: controlling myocardial inflammatory responses. *Annu. Rev. Physiol.* **68**, 67-95 (2006).

20 Knuefermann, P., Vallejo, J. & Mann, D. L. The role of innate immune responses in the heart in health and disease. *Trends in cardiovascular medicine* **14**, 1-7 (2004).

21 Song, X., Kusakari, Y., Xiao, C.-Y., Kinsella, S. D., Rosenberg, M. A., Scherrer-Crosbie, M., Hara, K., Rosenzweig, A. & Matsui, T. mTOR attenuates the inflammatory response in cardiomyocytes and prevents cardiac dysfunction in pathological hypertrophy. *American Journal of Physiology-Cell Physiology* **299**, C1256-C1266 (2010).

22 Xia, Y., Lee, K., Li, N., Corbett, D., Mendoza, L. & Frangogiannis, N. G. Characterization of the inflammatory and fibrotic response in a mouse model of cardiac pressure overload. *Histochemistry and cell biology* **131**, 471-481 (2009).

23 Mouton, A. J., Li, X., Hall, M. E. & Hall, J. E. Obesity, hypertension, and cardiac dysfunction: Novel roles of immunometabolism in macrophage activation and inflammation. *Circulation Research* **126**, 789-806 (2020).

24 Salvador, A. M., Nevers, T., Velázquez, F., Aronovitz, M., Wang, B., Abadía Molina, A., Jaffe, I. Z., Karas, R. H., Blanton, R. M. & Alcaide, P. Intercellular adhesion molecule 1 regulates left ventricular leukocyte infiltration, cardiac remodeling, and function in pressure overload–induced heart failure. *Journal of the American Heart Association* **5**, e003126 (2016).

25 Damilano, F., Franco, I., Perrino, C., Schaefer, K., Azzolino, O., Carnevale, D., Cifelli, G., Carullo, P., Ragona, R. & Ghigo, A. Distinct effects of leukocyte and cardiac phosphoinositide 3-kinase γ activity in pressure overload–induced cardiac failure. *Circulation* **123**, 391-399 (2011).

26 Weisheit, C., Zhang, Y., Faron, A., Köpke, O., Weisheit, G., Steinsträsser, A., Frede, S., Meyer, R., Boehm, O. & Hoeft, A. Ly6C low and not Ly6C high macrophages accumulate first in the heart in a model of murine pressure-overload. *PloS one* **9**, e112710 (2014).

27 Nevers, T., Salvador, A. M., Grodecki-Pena, A., Knapp, A., Velázquez, F., Aronovitz, M., Kapur, N. K., Karas, R. H., Blanton, R. M. & Alcaide, P. Left ventricular T-cell recruitment contributes to the pathogenesis of heart failure. *Circulation: Heart Failure* **8**, 776-787 (2015).

28 Laroumanie, F., Douin-Echinard, V., Pozzo, J., Lairez, O., Tortosa, F., Vinel, C., Delage, C., Calise, D., Dutaur, M. & Parini, A. CD4+ T cells promote the transition from hypertrophy to heart failure during chronic pressure overload. *Circulation* **129**, 2111-2124 (2014).

29 Chen, B. & Frangogiannis, N. G. The role of macrophages in nonischemic heart failure. *JACC: Basic to Translational Science* **3**, 245 (2018).

30 Roe, N. D., Standage, S. W. & Tian, R. (Am Heart Assoc, 2016).

31 Drosatos, K., Pollak, N. M., Pol, C. J., Ntziachristos, P., Willecke, F., Valenti, M.-C., Trent, C. M., Hu, Y., Guo, S. & Aifantis, I. Cardiac myocyte KLF5 regulates Ppara expression and cardiac function. *Circulation research* **118**, 241-253 (2016).

32 Ichihara, S., Obata, K., Yamada, Y., Nagata, K., Noda, A., Ichihara, G., Yamada, A., Kato, T., Izawa, H. & Murohara, T. Attenuation of cardiac dysfunction by a PPAR-α agonist is associated with down-regulation of redox-regulated transcription factors. *Journal of Molecular and Cellular Cardiology* **41**, 318-329 (2006).

33 Watanabe, K., Fujii, H., Takahashi, T., Kodama, M., Aizawa, Y., Ohta, Y., Ono, T., Hasegawa, G., Naito, M. & Nakajima, T. Constitutive regulation of cardiac fatty acid metabolism through peroxisome proliferator-activated receptor α associated with age-dependent cardiac toxicity. *Journal of Biological Chemistry* **275**, 22293-22299 (2000).

34 Campbell, F. M., Kozak, R., Wagner, A., Altarejos, J. Y., Dyck, J. R., Belke, D. D., Severson, D. L., Kelly, D. P. & Lopaschuk, G. D. A role for peroxisome proliferator-activated receptor α (PPARα) in the control of cardiac malonyl-CoA levels reduced fatty acid oxidation rates and increased glucose oxidation rates in the hearts of mice lacking PPARα are associated with higher concentrations of malonyl-coa and reduced expression of malonyl-CoA decarboxylase. *Journal of Biological Chemistry* **277**, 4098-4103 (2002).

35 Goikoetxea, M. J., Beaumont, J. & Díez, J. D. Peroxisome proliferator-activated receptor α and hypertensive heart disease. *Drugs* **64**, 9-18 (2004).

36 Iglarz, M., Touyz, R. M., Amiri, F., Lavoie, M.-F., Diep, Q. N. & Schiffrin, E. L. Effect of peroxisome proliferator–activated receptor-α and-γ activators on vascular remodeling in endothelin-dependent hypertension. *Arteriosclerosis, thrombosis, and vascular biology* **23**, 45-51 (2003).

37 Poynter, M. E. & Daynes, R. A. Peroxisome proliferator-activated receptor α activation modulates cellular redox status, represses nuclear factor-κB signaling, and reduces inflammatory cytokine production in aging. *Journal of biological chemistry* **273**, 32833-32841 (1998).

38 Jia, Z., Xue, R., Liu, G., Li, L., Yang, J., Pi, G., Ma, S. & Kan, Q. HMGB1 is involved in the protective effect of the PPARα agonist fenofibrate against cardiac hypertrophy. *PPAR research* **2014** (2014).

39 Kaimoto, S., Hoshino, A., Ariyoshi, M., Okawa, Y., Tateishi, S., Ono, K., Uchihashi, M., Fukai, K., Iwai-Kanai, E. & Matoba, S. Activation of PPAR-α in the early stage of heart failure maintained myocardial function and energetics in pressure-overload heart failure. *American Journal of Physiology-Heart and Circulatory Physiology* **312**, H305-H313 (2017).

40 Khuchua, Z., Glukhov, A. I., Strauss, A. W. & Javadov, S. Elucidating the beneficial role of PPAR agonists in cardiac diseases. *International journal of molecular sciences* **19**, 3464 (2018).

41 Lecarpentier, Y., Claes, V., Duthoit, G. & Hébert, J.-L. Circadian rhythms, Wnt/beta-catenin pathway and PPAR alpha/gamma profiles in diseases with primary or secondary cardiac dysfunction. *Frontiers in physiology* **5**, 429 (2014).

42 Goodwin, G. W., Taylor, C. S. & Taegtmeyer, H. Regulation of energy metabolism of the heart during acute increase in heart work. *Journal of Biological Chemistry* **273**, 29530-29539 (1998).

43 Karwi, Q. G., Uddin, G. M., Ho, K. L. & Lopaschuk, G. D. Loss of metabolic flexibility in the failing heart. *Frontiers in cardiovascular medicine* **5**, 68 (2018).

44 Noordali, H., Loudon, B. L., Frenneaux, M. P. & Madhani, M. Cardiac metabolism—a promising therapeutic target for heart failure. *Pharmacology & therapeutics* **182**, 95-114 (2018).

45 Sambandam, N., Lopaschuk, G. D., Brownsey, R. W. & Allard, M. F. Energy metabolism in the hypertrophied heart. *Heart failure reviews* **7**, 161-173 (2002).
46 Smith, R. L., Soeters, M. R., Wüst, R. C. & Houtkooper, R. H. Metabolic flexibility as an adaptation to energy resources and requirements in health and disease. *Endocrine reviews* **39**, 489-517 (2018).
47 Lin, J., Chang, R., Chen, Y., Yang, J., Baskaran, R., Chung, L., Chen, R., Day, C., Vijaya Padma, V. & Huang, C. Beta-catenin overexpression causes an increase in inflammatory cytokines and NF-kappaB activation in cardiomyocytes. *Cell Mol Biol (Noisy-le-grand)* **63**, 17-22 (2016).
48 Jang, J., Jung, Y., Chae, S., Chung, S.-I., Kim, S.-M. & Yoon, Y. Wnt/β-catenin pathway modulates the tnf-α-induced inflammatory response in bronchial epithelial cells. *Biochemical and biophysical research communications* **484**, 442-449 (2017).
49 Zhao, Y., Wang, C., Wang, C., Hong, X., Miao, J., Liao, Y., Zhou, L. & Liu, Y. An essential role for Wnt/β-catenin signaling in mediating hypertensive heart disease. *Scientific reports* **8**, 1-14 (2018).
50 Deb, A. Cell–cell interaction in the heart via Wnt/β-catenin pathway after cardiac injury. *Cardiovascular research* **102**, 214-223 (2014).
51 Zhou, D., Tan, R. J., Fu, H. & Liu, Y. Wnt/β-catenin signaling in kidney injury and repair: a double-edged sword. *Laboratory Investigation* **96**, 156-167 (2016).
52 Sasaki, T., Hwang, H., Nguyen, C., Kloner, R. A. & Kahn, M. The small molecule Wnt signaling modulator ICG-001 improves contractile function in chronically infarcted rat myocardium. *PloS one* **8**, e75010 (2013).
53 Zhao, Y., Wang, C., Hong, X., Miao, J., Liao, Y., Hou, F. F., Zhou, L. & Liu, Y. Wnt/β-catenin signaling mediates both heart and kidney injury in type 2 cardiorenal syndrome. *Kidney international* **95**, 815-829 (2019).
54 Sato, T., Sato, C., Kadowaki, A., Watanabe, H., Ho, L., Ishida, J., Yamaguchi, T., Kimura, A., Fukamizu, A. & Penninger, J. M. ELABELA-APJ axis protects from pressure overload heart failure and angiotensin II-induced cardiac damage. *Cardiovascular Research* **113**, 760-769 (2017).
55 Wang, Z., Xu, Y., Wang, M., Ye, J., Liu, J., Jiang, H., Ye, D. & Wan, J. TRPA1 inhibition ameliorates pressure overload-induced cardiac hypertrophy and fibrosis in mice. *EBioMedicine* **36**, 54-62 (2018).
56 Patel, B., Bansal, S. S., Ismahil, M. A., Hamid, T., Rokosh, G., Mack, M. & Prabhu, S. D. CCR2+ monocyte-derived infiltrating macrophages are required for adverse cardiac remodeling during pressure overload. *JACC: Basic to Translational Science* **3**, 230-244 (2018).
57 Drosatos, K., Khan, R. S., Trent, C. M., Jiang, H., Son, N.-H., Blaner, W. S., Homma, S., Schulze, P. C. & Goldberg, I. J. PPARγ activation prevents sepsis-related cardiac dysfunction and mortality in mice: drosatos et al: PPARγ treats septic cardiac dysfunction. *Circulation. Heart failure* **6**, 550 (2013).
58 Xiao, L., Zhou, D., Tan, R. J., Fu, H., Zhou, L., Hou, F. F. & Liu, Y. Sustained activation of Wnt/β-catenin signaling drives AKI to CKD progression. *Journal of the American Society of Nephrology* **27**, 1727-1740 (2016).
59 Li, C., Sun, X.-N., Zeng, M.-R., Zheng, X.-J., Zhang, Y.-Y., Wan, Q., Zhang, W.-C., Shi, C., Du, L.-J. & Ai, T.-J. Mineralocorticoid Receptor Deficiency in T Cells Attenuates Pressure Overload–Induced Cardiac Hypertrophy and Dysfunction Through Modulating T-

Cell Activation. *Hypertension* **70**, 137-147 (2017).
60 Wang, H., Kwak, D., Fassett, J., Hou, L., Xu, X., Burbach, B. J., Thenappan, T., Xu, Y., Ge, J.-b. & Shimizu, Y. CD28/B7 deficiency attenuates systolic overload-induced congestive heart failure, myocardial and pulmonary inflammation, and activated T cell accumulation in the heart and lungs. *Hypertension* **68**, 688-696 (2016).
61 Schulze, P. C. & Lee, R. T. (Am Heart Assoc, 2004).
62 Henderson, W. R., Chi, E. Y., Ye, X., Nguyen, C., Tien, Y.-t., Zhou, B., Borok, Z., Knight, D. A. & Kahn, M. Inhibition of Wnt/β-catenin/CREB binding protein (CBP) signaling reverses pulmonary fibrosis. *Proceedings of the National Academy of Sciences* **107**, 14309-14314 (2010).
63 Zhou, D., Fu, H., Zhang, L., Zhang, K., Min, Y., Xiao, L., Lin, L., Bastacky, S. I. & Liu, Y. Tubule-derived Wnts are required for fibroblast activation and kidney fibrosis. *Journal of the American Society of Nephrology* **28**, 2322-2336 (2017).
64 van de Schans, V. A., van den Borne, S. W., Strzelecka, A. E., Janssen, B. J., van der Velden, J. L., Langen, R. C., Wynshaw-Boris, A., Smits, J. F. & Blankesteijn, W. M. Interruption of Wnt signaling attenuates the onset of pressure overload-induced cardiac hypertrophy. *Hypertension* **49**, 473-480 (2007).
65 Laeremans, H., Hackeng, T. M., van Zandvoort, M. A., Thijssen, V. L., Janssen, B. J., Ottenheijm, H. C., Smits, J. F. & Blankesteijn, W. M. Blocking of frizzled signaling with a homologous peptide fragment of wnt3a/wnt5a reduces infarct expansion and prevents the development of heart failure after myocardial infarction. *Circulation* **124**, 1626-1635 (2011).
66 Ishida, H., Kogaki, S., Narita, J., Ichimori, H., Nawa, N., Okada, Y., Takahashi, K. & Ozono, K. LEOPARD-type SHP2 mutant Gln510Glu attenuates cardiomyocyte differentiation and promotes cardiac hypertrophy via dysregulation of Akt/GSK-3β/β-catenin signaling. *American Journal of Physiology-Heart and Circulatory Physiology* **301**, H1531-H1539 (2011).
67 Xiang, F.-L., Fang, M. & Yutzey, K. E. Loss of β-catenin in resident cardiac fibroblasts attenuates fibrosis induced by pressure overload in mice. *Nature communications* **8**, 1-12 (2017).
68 Haq, S., Michael, A., Andreucci, M., Bhattacharya, K., Dotto, P., Walters, B., Woodgett, J., Kilter, H. & Force, T. Stabilization of β-catenin by a Wnt-independent mechanism regulates cardiomyocyte growth. *Proceedings of the National Academy of Sciences* **100**, 4610-4615 (2003).
69 Emami, K. H., Nguyen, C., Ma, H., Kim, D. H., Jeong, K. W., Eguchi, M., Moon, R. T., Teo, J.-L., Oh, S. W. & Kim, H. Y. A small molecule inhibitor of β-catenin/cyclic AMP response element-binding protein transcription. *Proceedings of the National Academy of Sciences* **101**, 12682-12687 (2004).
70 Du, X. J. Divergence of hypertrophic growth and fetal gene profile: the influence of β-blockers. *British journal of pharmacology* **152**, 169-171 (2007).
71 Angrisano, T., Schiattarella, G. G., Keller, S., Pironti, G., Florio, E., Magliulo, F., Bottino, R., Pero, R., Lembo, F. & Avvedimento, E. V. Epigenetic switch at atp2a2 and myh7 gene promoters in pressure overload-induced heart failure. *PLoS One* **9**, e106024 (2014).
72 Sun, S., Kee, H. J., Ryu, Y., Choi, S. Y., Kim, G. R., Kim, H.-S., Kee, S.-J. & Jeong, M. H. Gentisic acid prevents the transition from pressure overload-induced cardiac hypertrophy to heart failure. *Scientific reports* **9**, 1-14 (2019).

73 Manabe, I., Shindo, T. & Nagai, R. Gene expression in fibroblasts and fibrosis: involvement in cardiac hypertrophy. *Circulation research* **91**, 1103-1113 (2002).
74 Roehlen, N., Crouchet, E. & Baumert, T. F. Liver Fibrosis: Mechanistic Concepts and Therapeutic Perspectives. *Cells* **9**, 875 (2020).
75 Akcora, B. Ö., Storm, G. & Bansal, R. Inhibition of canonical WNT signaling pathway by β-catenin/CBP inhibitor ICG-001 ameliorates liver fibrosis in vivo through suppression of stromal CXCL12. *Biochimica et Biophysica Acta (BBA)-Molecular Basis of Disease* **1864**, 804-818 (2018).
76 Meng, X.-m., Nikolic-Paterson, D. J. & Lan, H. Y. TGF-β: the master regulator of fibrosis. *Nature Reviews Nephrology* **12**, 325 (2016).
77 Shah, R., Coelho-Filho, O. R., Mitchell, R. N., Kwong, R. Y., Das, S., Rosenzweig, A. & Jerosch-Herold, M. Cellular hypertrophy occurs before interstitial fibrosis in pressure-overload heart failure. *Journal of Cardiovascular Magnetic Resonance* **15**, 1-2 (2013).
78 Muta, K., Nakazawa, Y., Obata, Y., Inoue, H., Torigoe, K., Nakazawa, M., Abe, K., Furusu, A., Miyazaki, M. & Yamamoto, K. An inhibitor of Krüppel-like factor 5 suppresses peritoneal fibrosis in mice. *Peritoneal Dialysis International*, 0896860820981322 (2021).
79 Li, Z. L., Lv, L. L., Wang, B., Tang, T. T., Feng, Y., Cao, J. Y., Jiang, L. Q., Sun, Y. B., Liu, H. & Zhang, X. L. The profibrotic effects of MK-8617 on tubulointerstitial fibrosis mediated by the KLF5 regulating pathway. *The FASEB Journal* **33**, 12630-12643 (2019).
80 Fujiu, K., Manabe, I. & Nagai, R. (Am Heart Assoc, 2009).
81 Hofmann, U. & Frantz, S. Role of lymphocytes in myocardial injury, healing, and remodeling after myocardial infarction. *Circulation research* **116**, 354-367 (2015).
82 Frieler, R. A. & Mortensen, R. M. Immune cell and other noncardiomyocyte regulation of cardiac hypertrophy and remodeling. *Circulation* **131**, 1019-1030 (2015).
83 Kamo, T., Akazawa, H. & Komuro, I. Cardiac nonmyocytes in the hub of cardiac hypertrophy. *Circulation research* **117**, 89-98 (2015).
84 Wang, Y., Sano, S., Oshima, K., Sano, M., Watanabe, Y., Katanasaka, Y., Yura, Y., Jung, C., Anzai, A. & Swirski, F. K. Wnt5a-Mediated Neutrophil Recruitment Has an Obligatory Role in Pressure Overload–Induced Cardiac Dysfunction. *Circulation* **140**, 487-499 (2019).
85 Carrillo-Salinas, F. J., Ngwenyama, N., Anastasiou, M., Kaur, K. & Alcaide, P. Heart inflammation: immune cell roles and roads to the heart. *The American journal of pathology* **189**, 1482-1494 (2019).
86 Ma, X.-L., Lin, Q.-Y., Wang, L., Xie, X., Zhang, Y.-L. & Li, H.-H. Rituximab prevents and reverses cardiac remodeling by depressing B cell function in mice. *Biomedicine & Pharmacotherapy* **114**, 108804 (2019).
87 Mouton, A. J., DeLeon-Pennell, K. Y., Gonzalez, O. J. R., Flynn, E. R., Freeman, T. C., Saucerman, J. J., Garrett, M. R., Ma, Y., Harmancey, R. & Lindsey, M. L. Mapping macrophage polarization over the myocardial infarction time continuum. *Basic research in cardiology* **113**, 26 (2018).
88 Liao, X., Shen, Y., Zhang, R., Sugi, K., Vasudevan, N. T., Alaiti, M. A., Sweet, D. R., Zhou, L., Qing, Y. & Gerson, S. L. Distinct roles of resident and nonresident macrophages in nonischemic cardiomyopathy. *Proceedings of the National Academy of Sciences* **115**, E4661-E4669 (2018).
89 Tsutsui, H., Isobe, M., Ito, H., Okumura, K., Ono, M., Kitakaze, M., Kinugawa, K., Kihara, Y., Goto, Y. & Komuro, I. JCS 2017/JHFS 2017 Guideline on Diagnosis and Treatment of Acute and Chronic Heart Failure—Digest Version—. *Circulation Journal* **83**, 2084-2184

(2019).
90 Wrigley, B. J., Lip, G. Y. & Shantsila, E. The role of monocytes and inflammation in the pathophysiology of heart failure. *European journal of heart failure* **13**, 1161-1171 (2011).
91 Dong, Z., Zhao, P., Xu, M., Zhang, C., Guo, W., Chen, H., Tian, J., Wei, H. & Cao, T. Astragaloside IV alleviates heart failure via activating PPARα to switch glycolysis to fatty acid β-oxidation. *Scientific reports* **7**, 1-15 (2017).
92 Warren, J. S., Oka, S.-i., Zablocki, D. & Sadoshima, J. Metabolic reprogramming via PPARα signaling in cardiac hypertrophy and failure: from metabolomics to epigenetics. *American Journal of Physiology-Heart and Circulatory Physiology* **313**, H584-H596 (2017).
93 Sansbury, B. E., DeMartino, A. M., Xie, Z., Brooks, A. C., Brainard, R. E., Watson, L. J., DeFilippis, A. P., Cummins, T. D., Harbeson, M. A. & Brittian, K. R. Metabolomic analysis of pressure-overloaded and infarcted mouse hearts. *Circulation: heart failure* **7**, 634-642 (2014).
94 Barger, P. M., Brandt, J. M., Leone, T. C., Weinheimer, C. J. & Kelly, D. P. Deactivation of peroxisome proliferator–activated receptor-α during cardiac hypertrophic growth. *The Journal of clinical investigation* **105**, 1723-1730 (2000).
95 Lai, L., Leone, T. C., Keller, M. P., Martin, O. J., Broman, A. T., Nigro, J., Kapoor, K., Koves, T. R., Stevens, R. & Ilkayeva, O. R. Energy metabolic reprogramming in the hypertrophied and early stage failing heart: a multisystems approach. *Circulation: Heart Failure* **7**, 1022-1031 (2014).
96 Ritterhoff, J., Young, S., Villet, O., Shao, D., Neto, F. C., Bettcher, L. F., Hsu, Y.-W. A., Kolwicz Jr, S. C., Raftery, D. & Tian, R. Metabolic Remodeling promotes cardiac hypertrophy by directing glucose to aspartate biosynthesis. *Circulation Research* **126**, 182-196 (2020).
97 Umbarawan, Y., Syamsunarno, M. R. A., Koitabashi, N., Obinata, H., Yamaguchi, A., Hanaoka, H., Hishiki, T., Hayakawa, N., Sano, M. & Sunaga, H. Myocardial fatty acid uptake through CD36 is indispensable for sufficient bioenergetic metabolism to prevent progression of pressure overload-induced heart failure. *Scientific reports* **8**, 1-13 (2018).
98 AbdAlla, S., Fu, X., S Elzahwy, S., Klaetschke, K., Streichert, T. & Quitterer, U. Up-regulation of the cardiac lipid metabolism at the onset of heart failure. *Cardiovascular & Hematological Agents in Medicinal Chemistry (Formerly Current Medicinal Chemistry-Cardiovascular & Hematological Agents)* **9**, 190-206 (2011).
99 van der Pol, A., van Gilst, W. H., Voors, A. A. & van der Meer, P. Treating oxidative stress in heart failure: past, present and future. *European journal of heart failure* **21**, 425-435 (2019).
100 Gyurászová, M., Kovalčíková, A., Janšáková, K., Šebeková, K., Celec, P. & Tóthová, Ľ. Markers of oxidative stress and antioxidant status in the plasma, urine and saliva of healthy mice. *Physiological Research* **67**, 921 (2018).
101 Hill, M. F., Palace, V. P., Kaur, K., Kumar, D., Khaper, N. & Singal, P. K. Reduction in oxidative stress and modulation of heart failure subsequent to myocardial infarction in rats. *Experimental & Clinical Cardiology* **10**, 146 (2005).
102 Sun, H. & Wang, Y. Branched chain amino acid metabolic reprogramming in heart failure. *Biochimica et Biophysica Acta (BBA)-Molecular Basis of Disease* **1862**, 2270-2275 (2016).
103 Zhang, S., Zeng, X., Ren, M., Mao, X. & Qiao, S. Novel metabolic and physiological functions of branched chain amino acids: a review. *Journal of animal science and*

*biotechnology* **8**, 10 (2017).

104 Chen, M., Gao, C., Yu, J., Ren, S., Wang, M., Wynn, R. M., Chuang, D. T., Wang, Y. & Sun, H. Therapeutic Effect of Targeting Branched-Chain Amino Acid Catabolic Flux in Pressure-Overload Induced Heart Failure. *Journal of the American Heart Association* **8**, e011625 (2019).

105 Mahmod, M., Pal, N., Rayner, J., Holloway, C., Raman, B., Dass, S., Levelt, E., Ariga, R., Ferreira, V. & Banerjee, R. The interplay between metabolic alterations, diastolic strain rate and exercise capacity in mild heart failure with preserved ejection fraction: a cardiovascular magnetic resonance study. *Journal of Cardiovascular Magnetic Resonance* **20**, 1-10 (2018).